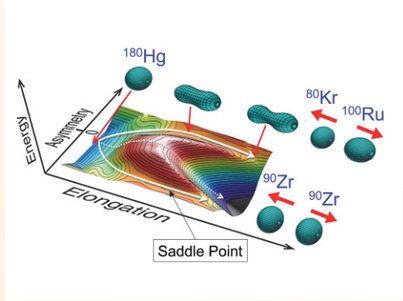

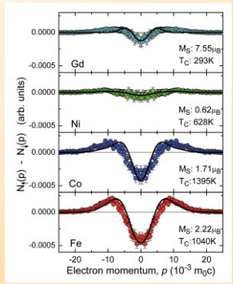

Annual Report of ASRC 2010►2011

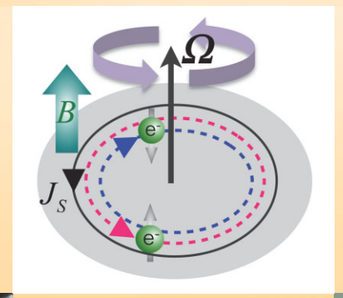

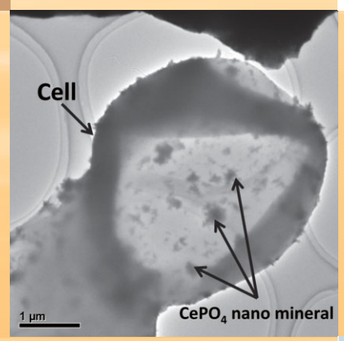

Japan Atomic Energy Agency

Advanced Science Research Center

2-4 Shirakata Shirane, Tokai-mura, Naka-gun, Ibaraki Pref. 319-1195
http://asrc.jaea.go.jp/asr_eng/

Advanced Science Research Center
Japan Atomic Energy Agency

Preface

Sadamichi Maekawa
Director General of Advanced Science Research Center

On behalf of the Advanced Science Research Center (ASRC), the Japan Atomic Energy Agency (JAEA), I would like to express my sincere sympathy to the people affected by the earthquake on March 11, 2011.

Some of the research facilities of JAEA have been damaged by the earthquake, and are now being restored. Fortunately, all the members of ASRC are fine and there is no harmful impact on the ASRC building. Although some of the experimental labs need some time to recover completely, the ASRC has returned to normal since March 22. The ASRC staffs are also making contributions to the JAEA's activities to deal with the Fukushima nuclear crisis. Despite the circumstances, the members have made good progress in their research. This is the issue of the Annual Report of ASRC's research activities focused in the fiscal year 2010, which includes six research highlights in ASRC and the summary of the research contents of 11 research groups.

July 2011

Pictures on Cover Page:

❶Potential energy of ^{180}Hg having the largest proton to neutron ratio among isotopes whose fission property was measured so far.

❷Czochralski-pulling method and a single crystal of high-quality URu_2Si_2.

❸Differential DBAR spectra of the Fe, Co, Ni and Gd samples obtained in the external magnetic field of 1 T at room temperature.

❹Schematic illustration of electrons' trajectories under mechanical rotation Ω and a magnetic field B. The circular spin current is generated in the uniformly rotating body.

❺TEM image of yeast cells after exposure to 1×10^{-4} mole/L Ce solution. $CePO_4$ nano minerals were developed directly from cell surface.

❻1st ASRC international workshop held in February 2011: Discussions at coffee break.

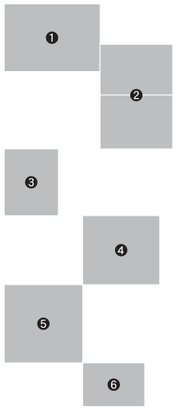

Contents

Strategy of Research

Sadamichi Maekawa

The Advanced Science Research Center (ASRC) has been conducting new frontier research related to atomic energy sciences. Our task is to discover new principles and phenomena with the advantages of the state-of-the-art research infrastructure of the Japan Atomic Energy Agency (JAEA). The subjects are carefully selected on the basis of their originality, as well as their scientific and technological potential impact. The research duration is limited to a maximum of five years. The strategy of research has been examined and approved at the Evaluation Committee of Research Activities for Advanced Science Research (an external committee) meeting, which was held in April 22-23, 2010.

The ASRC runs with the following three visions:

1. To pursue advanced basic research,
2. To be an international center of excellence (COE) for basic research in atomic energy sciences,
3. To develop new research fields and foster talented young scientists.

Toward the international COE:

The ASRC promotes the following programs;

i) Appointment of two distinguished scientists as the research advisors.

ii) Invitation of three world-wide leading scientists as the group leaders.

iii) Conducting international collaborations through the Reimei Research Program (a funding program of ASRC).

iv) Organization of Evaluation Committee to review ASRC from the international viewpoint.

Research programs:

The following three research areas are taken up at the fiscal year 2010, and each area has several advanced research subjects;

i) Advanced materials research.

ii) Frontier research on heavy element systems.

iii) Research on radiation field effects.

Organization of ASRC

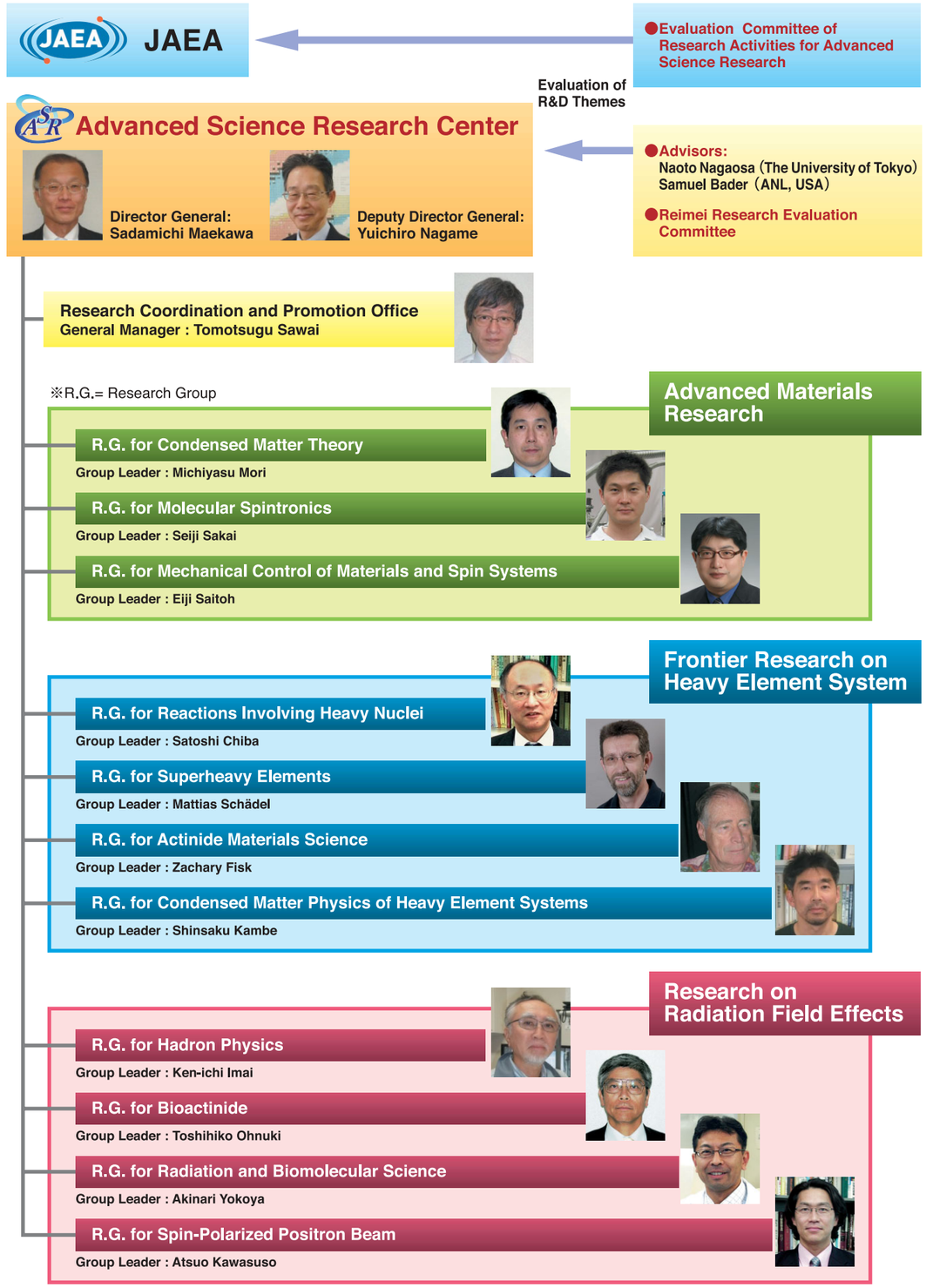

Effects of mechanical rotation on spin currents

M. Matsuo[1,2], J. Ieda[1,3], E. Saitoh[3,4,5], and S. Maekawa[1,3]
1) R.G. for Condensed Matter Theory, ASRC, JAEA 2) Kyoto University 3) CREST, JST
4) R.G. for Mechanical Control of Materials and Spin Systems, ASRC, JAEA 5) Tohoku University

In 1915, Albert Einstein, Wander Johannes de Haas and Samuel Jackson Barnet discovered the coupling of magnetism and rotational motion [1,2]. They measured the gyromagnetic ratio and the anomalous g factor of electrons well before the dawn of modern quantum physics. Recent developments in nanoprocessing technologies have led to the detection of the effects of mechanical rotation on nanostructured magnetic systems [3, 4].

Spin-dependent transport phenomena in magnetic nanostructures are of great interest in the field of spintronics, i.e. the study of "spin current" or flow of spins. One of the more intense research areas concerns the coupling of the magnetization and spin current leading to such phenomena as spin transfer torque [5,6], spin pumping [7], and spin motive force [8].

Comparing to the well-established coupling of mechanical rotations and magnetization, and that of magnetization and spin currents, the direct coupling of mechanical rotations and spin currents has not been demonstrated so far. Our purpose is to link the mechanical rotation with spin currents (Fig. 1).

We derived the fundamental Hamiltonian with a direct coupling of spin currents and mechanical rotations from the general relativistic Dirac equation [9]. The introduction of mechanical rotations involves extending our physical system from an inertial to noninertial frame. The dynamics of spin currents is closely related to the spin-orbit interaction (SOI), which results from taking the low energy limit of the Dirac equation. We obtained the SOI in a uniformly rotating frame:

$$H_{SOI} = \frac{e\lambda}{\hbar}\boldsymbol{\sigma}\cdot\left(\mathbf{p}+e\mathbf{A}\right)\times\left(\mathbf{E}+\left(\boldsymbol{\Omega}\times\mathbf{r}\right)\times\mathbf{B}\right)$$

where $\boldsymbol{\Omega}$ is rotation frequency, $\mathbf{E}$ and $\mathbf{B}$ are applied electric and magnetic fields, $\mathbf{A}$ is a vector potential, σ is the spin operator of electron and λ is the spin-orbit coupling. This new term responsible for the spin current generation arising from mechanical rotation.

To clarify physical meanings of the SOI, we investigate the semiclassical equation of motion for electron. Choosing $\mathbf{E}$=0, $\mathbf{B}$=(0,0,B), and $\boldsymbol{\Omega}$=(0,0,Ω), we have the spin-dependent velocity of electron:

$$\mathbf{v} = \dot{\mathbf{r}} + \mathbf{v}_\sigma, \quad \mathbf{v}_\sigma = \left(e\lambda/\hbar\right)\boldsymbol{\sigma}\times B\Omega\mathbf{r}.$$

The first term is conventional velocity of electron. The second term, $\mathbf{v}_\sigma$ is so-called anomalous velocity, i.e., the spin-dependent velocity. The z-polarized spin current J_s can be estimated by

$$J_s = ne\mathrm{Tr}\sigma_z\mathbf{v} = \left(2ne\lambda B\Omega r/\hbar\right)\mathbf{e}_\phi,$$

where n is the density of electron and $\mathbf{e}_\phi$ is the azimuthal unit vector. The magnitude of the spin current is linearly proportional to the angular velocity of the mechanical rotation, a magnetic field, and the spin-orbit coupling strength. The formula above reveals a mechanism for the quantum mechanical transfer of angular momentum between a rigid rotation and a spin current. The z-polarized spin current is created in the azimuthal direction by the mechanical rotation (Fig. 2). In the case of B=1 T, Ω=1 kHz, r=10^{-1} m, $\lambda = 0.6\times10^{20}$ m^{-2} [10], the spin current becomes J_s~10^8 A/m^2. This can be investigated using spin detection methods such as nonlocal spin valves [11], the inverse spin Hall effect [12] and the real-time imaging method [13].

It should be noted that starting from the general relativistic Dirac equation is essential when treating spintronic phenomena in accelerating frames. The present formalism [9] offers a route to "spin mechatronics", viz., a strong coupling of mechanical motion with spin and charge transport in nanostructures. Our findings will be experimentally examined by R.G. for Mechanical control of materials and spin systems.

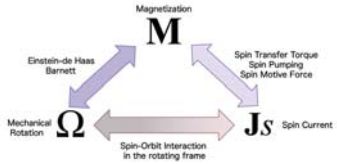

Fig. 1 Angular momentum transfers between interacting systems.

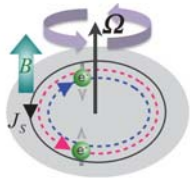

Fig. 2 Schematic illustration of electrons' trajectories under mechanical rotation Ω and a magnetic field **B**. The circular spin current is generated in the uniformly rotating body.

References

[1] A. Einstein *et al.*, Verh. Dtsch. Phys. Ges. **17**, 152 (1915).
[2] S. J. Barnett, Phys. Rev. **6**, 239 (1915).
[3] T. M. Wallis *et al.*, Appl. Phys. Lett. **89**, 122502 (2006).
[4] G. Zolfagharkhani *et al.*, Nat. Nanotechnol. **3**, 720 (2008).
[5] J. C. Slonczewski, J. Magn. Magn. Mater. **159**, L1 (1996).
[6] L. Berger, Phys. Rev. B **54**, 9353 (1996).
[7] Y. Tserkovnyak *et al.*, Phys. Rev. Lett. **88**, 117601 (2002).
[8] S. E. Barnes *et al.*, Phys. Rev. Lett. **98**, 246601 (2007).
[9] M. Matsuo *et al.*, Phys. Rev. Lett. **106**, 076601 (2011).
[10] L. Vila *et al.*, Phys. Rev. Lett. **99**, 226604 (2007).
[11] T. Yang *et al.*, Nature Phys. **4**, 851 (2008).
[12] E. Saitoh *et al.*, Appl. Phys. Lett. **88**, 182509 (2006).
[13] L. K. Werake *et al.*, Nature Phys. **6**, 875 (2010).

New type of asymmetric fission in proton-rich nucleus ^{180}Hg

K. Nishio[1] and A. N. Andreyev[2] for collaboration of University of the West of Scotland, JAEA, Katholieke Universiteit Leuven, Commenius University, Petersburg nuclear physics institute, GSI, CERN-ISOLDE, University of Paris Sud, ILL, University of Liverpool, University of Ioannina, University of Manchester, University of Gent, Slovak Academy of Science, Yukawa Institute for Theoretical Physics, LANL
1) R.G for Reactions Involving Heavy Nuclei, ASRC, JAEA 2) University of the West of Scotland

From the discovery of nuclear fission [1], extensive measurements have been done to understand this dramatic phenomenon in nucleus. An essential feature of the liquid-drop model [2] is that nucleus has a saddle point which is formed by the interplay between the attractive surface force and the repulsive Coulomb force. Fission proceeds when the excitation energy of a compound nucleus is higher than the saddle point. The classical model, however, cannot explain the important features of fission, such as mass asymmetric fission as observed in neutron-induced fission of ^{235}U. This necessitates the microscopic model (effects associated with shell structure) in fission. The effects of the doubly closed shells at ^{132}Sn play a role in the rupture process in the last stage of fission in such a way that the fragment in the vicinity of ^{132}Sn is preferentially formed.

The fission of a proton-rich nucleus like ^{180}Hg is free from the shells of ^{132}Sn due to largely different proton to neutron ratio of Z/N = 0.800 (^{180}Hg) from 0.610 (^{132}Sn). Instead, the fission would be influenced by the semi-magic nucleus ^{90}Zn (Z/N = 0.800), and thus the symmetric fission would be expected when we simply apply the current understanding in fission.

A β^+-decay delayed fission (βDF) gives an opportunity to observe fission for such a proton-rich nucleus. The excited daughter nucleus is formed by the β^+ decay with the maximum excitation energy corresponding to the Q value of the β^+ decay, Q_β. The fission takes place when the fission barrier height B_f is lower or nearly equal to Q_β. The first observation of βDF in proton-rich nucleus ^{180}Tl was reported in [3] where the βDF fragment is recorded as a track on a plastic plate. Instead, by using silicon detectors we observed large amplitude of pulse signals from both βDF fragments of ^{180}Hg (daughter of ^{180}Tl) in coincidence. Furthermore, we registered K X-ray of Hg in coincidence with fission fragments. They give a definite evidence for βDF. Using the pulse height (energy) of each fragment, we determined the mass division in the fission of ^{180}Hg.

The experiment was carried out at the ISOLDE mass separator at CERN. The ^{180}Tl was produced by using a 1.4 GeV proton beam impinging on a stack of UC_x targets. A laser ionization and mass separation are used to extract a pure ^{180}Tl ion beam. The ^{180}Tl$^+$ ions with 30 kV were implanted onto a thin carbon foil to detect βDF fragments.

Totally 346 events of coincided fragments were registered. The results are shown in Fig. 1, where the number of events is plotted as functions of mass and total kinetic energy (TKE) [4]. The spectrum clearly shows an asymmetric mass distribution with the most probable masses of A_H = 100(1) and A_L = 80(1) for heavy and light fragments, respectively. By assuming the Z/N ratio of the fragments to be equal to ^{180}Hg, the most probable isotopes become ^{100}Ru and ^{80}Kr. The average TKE of both fragments is determined to be 134.6(7) MeV.

The observed asymmetric fission in ^{180}Hg apparently contradicts the expected feature in fission built from the actinide fissions. The shells of fragments (^{90}Zr) do not play a role.

To understand this feature, we calculated a potential energy surface of ^{180}Hg as shown in Fig. 2 using a macroscopic-microscopic model where the effects of the shells are taken into account. It is found that the saddle point is located at the mass asymmetry of A_H/A_L = 108/72 with a fission barrier height B_f = 9.8 MeV. Considering Q_β = 10.4 MeV [5], fission proceeds only through the asymmetric saddle point. The result also shows a deep symmetric valley on the elongated nuclear shape, which linked to the shells of ^{90}Zr. The experiment reveals that the mass asymmetry in the fission of ^{180}Hg is fixed at the saddle point, and rearrangement of mass asymmetry does not occur in descending from the saddle to scission.

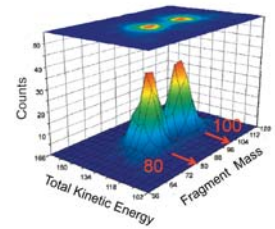

Fig. 1 Number of fission events plotted as functions of mass and total kinetic energy.

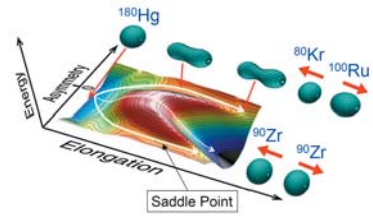

Fig. 2 Potential energy surface of ^{180}Hg. Saddle point is indicated.

References

[1] O. Hahn and F. Strassmann, Naturewissenschaften **27** 1, 11 (1939).
[2] N. Bohr and J. A. Wheeler, Phys. Rev. **56**, 426 (1939).
[3] Y. A. Lazarev *et al.*, Europhys. Lett. **4**, 893 (1987).
[4] A. N. Andreyev *et al.*, Phys. Rev. Lett. **105**, 252502 (2010).
[5] P. Möller *et al.*, Phys. Rev. C **79**, 064304 (2009).

Hidden-order state in URu_2Si_2 : High-quality single crystal and novel techniques

Y. Haga[1)], T. D. Matsuda[1)], E. Yamamoto[1)], Y. Ōnuki[1,2)], R. Yoshida[3)], Y. Nakamura[3)], M. Fukui[3)], M. Okawa[4)], S. Shin[4)], M. Hirai[3)], Y. Muraoka[3)], T. Yokoya[3)], R. Okazaki[5)], T. Shibauchi[5)], H. J. Shi[5)], H. Ikeda[5)], and Y. Matsuda[5)]
1) R.G for Actinide Materials, ASRC, JAEA 2) Osaka University 3) Okayama University
4) The University of Tokyo 5) Kyoto University

URu_2Si_2 is one of the heavy fermion compounds where the effective mass of the conduction electron is large compared to that of ordinary metals. This compound has been particularly investigated because of its remarkable features. One is the occurrence of superconductivity below 1.4 K where the 'heavy electrons' form Cooper pairs. Another one is a phase transition occurring at higher temperature 17.5 K. Early researches suggested this is due to a magnetic phase transition, because the 5*f* electrons carries magnetic moments and it is natural to assume that they order below the transition temperature. However, any efforts to detect the signature of the magnetic ordering have failed since its discovery in 1985 [1]. Other possibilities such as the ordering of multipolar moments of 5*f* electron were investigated but no clear evidence was found. The nature of the 'hidden-order' state is now one of the important subjects in condensed-matter physics.

To tackle this problem we carefully prepared a high quality single crystal of URu_2Si_2 to eliminate impurity effects which become significant at low-temperatures. Using the Czochralski pulling method and subsequent solid-state electrotransport annealing under ultra high vacuum [2], we succeeded to prepare an extremely pure single crystal. The purity of the metallic compound is measured by the residual resistivity ratio (RRR) where the residual resistivity at very low temperature reflects impurity concentration. Our sample shows RRR ~1000, much larger than the samples prepared by other researchers. Figure 1 shows the temperature dependence of electrical resistivity of URu_2Si_2 clearly showing the hidden-order transition at To =17.5 K and superconducting one at 1.4 K. Among the 5 samples, No. 1 shows the lowest residual resistivity. This single crystal was investigated further using two experimental techniques, high energy-resolution photoemission spectroscopy [3] and torque magnetometry using a micro cantilever [4].

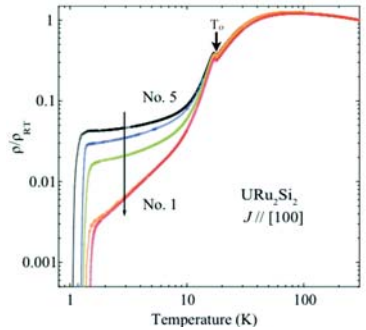

Fig. 1 Temperature dependence of electrical resistivity in URu_2Si_2.

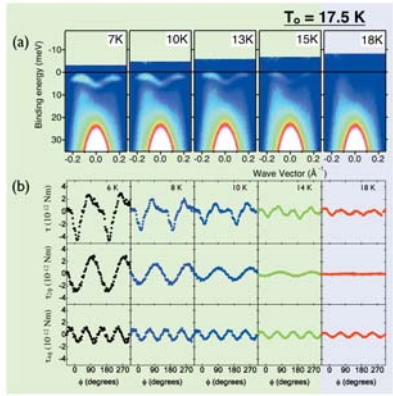

Fig. 2 (a) Photoemission spectra [3] and (b) magnetic torque [4] of URu_2Si_2 as a function of temperature.

The results are summarized in Fig. 2. Fig. 2(a) shows the intensity mapping of the photoelectron as functions of the binding energy and wave vector. At 18 K the spectrum consists of a strong intensity around 30 meV (originating from the surface effect) and hole band cutting the Fermi energy (E = 0 meV). On cooling below the transition temperature 17.5 K, a new feature appears around 2-5 meV. The intensity of the narrow band increases with decreasing temperature. Fig. 2(b) is the result of the magnetic torque measurements. The upper panels show the total magnetic anisotropy as a function of magnetic field angle within the tetragonal basal plane, while the middle and bottom panels correspond to the decomposed two-fold and four-fold components, respectively. Because of the tetragonal structure of URu_2Si_2, the magnetic anisotropy should follow the tetragonal (four-fold) rotational symmetry. Above 17.5 K, in fact, the magnetic torque can be expressed by a four-fold oscillation. However in the hidden-order state, a two-fold component, which breaks the crystal symmetry, appears.

These observations clearly demonstrate the emergence of a new electronic state in the hidden-order state and provide new insights for the exotic phase transition observed in highly correlated electron systems.

References

[1] T. T. M. Palstra *et al.*, Phys. Rev. Lett. **55**, 2727 (1985).
[2] T. D. Matsuda *et al.*, J. Phys. Soc. Jpn. **77** Suppl. A, 362 (2008).
[3] R. Yoshida *et al.*, Phys. Rev. B **82**, 205108 (2010).
[4] R. Okazaki *et al.*, Science **331**, 439 (2011).

A specific Ce anomaly during sorption of rare earth elements on biogenic Mn oxide produced by *Acremonium* sp. strain KR21-2

K. Tanaka[1,2)], Y. Tani[3)], Y. Takahashi[2)], M. Tanimizu[4)], Y. Suzuki[1,5)], N. Kozai[1)], T. Ohnuki[1)]
1) R.G. for Bioactinide, ASRC, JAEA 2) Hiroshima University 3) Shizuoka University
4) JAMSTEC 5) Tokyo University of Technology

Microbial oxidation of Mn(II) occurs at rates of up to 5 orders of magnitude greater than abiotic Mn(II) oxidation [1]. Mn(II)-oxidizing microorganisms are thought to play an important role in the formation of Mn oxides in most natural environments [2]. It is well known that oxidation of Ce(III) by synthetic Mn oxide causes Ce sorption anomaly in rare earth element (REE) partitioning pattern [3]. However, the sorption behavior of REE and Ce oxidation process by biogenic Mn oxide have not been clarified. In the present study, we examined the relevance of microorganisms to the Ce(III) oxidation process by biogenic Mn using *Acremonium* sp. strain KR21-2 [4]. To accomplish this, we made sorption experiments of REEs between biogenic Mn oxides and aqueous solution.

We used *Acremonium* sp. strain KR21-2 as a model of Mn-oxidizing fungi, as described above. The hyphae and biogenic Mn oxide were put into 100 mL of 10 mmol/L NaCl solution which contains 100 ng/mL REE each. The initial pH was then adjusted with NaOH and HCl solutions. Sample solutions after 25 h were collected by filtration with a 0.2 μm filter. REE concentrations in the solutions were determined with ICP-MS. We characterized REE species in the solutions using size exclusion column (SEC) HPLC-ICP-MS. Cerium L_{III}-edge X-ray absorption near edge structure (XANES) spectra were recorded at beamline 12C at the Photon Factory, KEK (Tsukuba, Japan), to determine the oxidation state of Ce sorbed on biogenic Mn oxide.

The distribution coefficient of REE, K_d(REE), between solid and solution is defined as the following equation: $K_d(REE) = ([REE]_{init} - [REE]_{fil})/c[REE]_{fil}$, where the term c (g/mL) is the ratio of solid to solution. The K_d(REE) patterns for the mixture of hyphae and biogenic Mn oxide (called biogenic Mn oxide hereinafter) at pH 3.83 showed a positive Ce anomaly, suggesting Ce(III) oxidation on biogenic Mn oxide (Fig. 1). Such large positive Ce anomaly was also reported in sorption of REE on abiotically synthesized Mn oxide [3]. The polarity of Ce anomaly shifted from positive to negative with increasing pH, and negative Ce anomaly was observed at pH 6.64 (Fig. 1), indicating Ce was preferentially remained in solution phase.

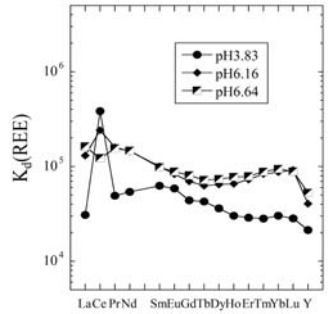

Fig. 1 K_d(REE) patterns at different pHs.

Cerium L_{III}-edge XANES spectra were shown in Fig. 2. The trivalent Ce reference species of $Ce_2(CO_3)_3{\cdot}8H_2O$ and the Ce(III) aqueous solution show a single white line peak at 5726 eV. In contrast, two distinct peaks were observed for the Ce(IV) compound of $Ce(SO_4)_2{\cdot}nH_2O$ around 5729 and 5737 eV. The XANES spectra of the Ce sorbed biogenic Mn oxide samples at pH 3.83, 6.16 and 6.64 show double white line peaks 5726 and 5737 eV. In particular, the second peak around 5737 eV common to the Ce(IV) references clearly indicates that Ce(III) was oxidized to Ce(IV) by the biogenic Mn oxide samples.

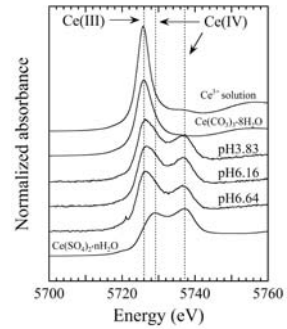

Fig. 2 Ce L_{III}-edge XANES spectra.

In the present study the positive Ce anomaly for the biogenic Mn oxide was observed at pH 3.83, and decreased with increasing pH (Fig. 1). Furthermore, negative Ce anomaly was observed at pH 6.64. The trend observed for our data is quite opposite to that observed for the previous studies using abiotically synthesized Mn oxide, where the degree of positive Ce anomaly increased with increasing pH [3]. The negative Ce anomaly indicates that a larger fraction of Ce was present in solution phase (i.e. < 0.2 μm fraction) than that of La and Pr (Fig. 1). SEC-HPLC-ICP-MS analysis demonstrated that the specific organic molecules had preferentially complexed with Ce(IV) in solution phase. A line of our data indicates that the negative Ce anomaly at pH 6.64 arose from Ce(III) oxidation on the biogenic Mn oxide and subsequent complexation of Ce(IV) with organic ligands released from fungal cells.

References

[1] B. Tebo *et al.*, *in Geomicrobiology: Interactions between microbes and minerals. Reviews in mineralogy,* ed. by J. F. Banfield and K. H. Nealson. (Mineralogical Society of America, Washington D.C., 1997), Vol. **35**, Chap. 7, p. 225.
[2] N. Mita *et al.*, Geochem. J. **28**, 71 (1994).
[3] A. Ohta and I. Kawabe, Geochim. Cosmochim. Acta **65**, 695 (2001).
[4] K. Tanaka *et al.*, Geochim. Cosmochim. Acta **74**, 5463 (2010).

Detection of excess electron spins in magnetic substances using highly spin-polarized positrons

A. Kawasuso[1)], M. Maekawa[1)], Y. Fukaya[1)], A. Yabuuchi[1)] , and I. Mochizuki[1)]
1) R.G. for Spin-polarized Positron Beam, ASRC, JAEA

We are currently developing a new utilization of the positron annihilation spectroscopy (PAS) in order to investigate magnetic materials and spin-related devices.

Generally, PAS technique is a powerful tool to detect atomic vacancies in crystalline solids. Positron annihilation lifetime and the Doppler effect on annihilation radiation energy spectrum are the observables in PAS measurement. The former is inversely proportional to electron density where positrons annihilate. The latter reflects electron momentum distribution. Very recently, we have successfully demonstrated a new feasibility of PAS using our built beam source of highly spin-polarized positron. Electron-positron annihilation characteristics depend on the spin state. A spin-singlet (S=0) electron-positron pair tends to self-annihilate (two-photon annihilation). The self-annihilation (three-photon annihilation) probability of a spin-triplet (S=1) electron-positron pair is much smaller than the pick-off annihilation probability with surrounding electrons. The above spin-dependent positron annihilation can be observed using spin-polarized positrons. That is, polarized electrons can be detected using spin-polarized positrons. This is the principle of spin-polarized positron annihilation spectroscopy (SP-PAS) [1].

Until now, the chief difficulty in SP-PAS is to obtain highly spin-polarized positrons. In this study, we have cleared up this difficulty to use a ^{68}Ge-^{68}Ga positron source that yields much highly spin-polarized positrons than the conventional ^{22}Na source [2]. To examine the feasibility of SP-PAS to apply any magnetic materials for the spin-electronic devices, we have performed the SP-PAS measurements of high quality for the simple ferromagnets (Fe, Co, Ni, and Gd). Figure 1 shows the differential Doppler broadening of annihilation radiation (DBAR) spectra between positive and negative magnetic field with respect to positron spin direction obtained for polycrystalline Fe, Co, Ni and Gd. The residuals are not zero. This is called field-reversal asymmetry.

Roughly speaking, the field-reversal asymmetry appears due to enhanced annihilation between spin-up positrons and spin-down 3*d*, 4*s* (Fe, Co, Ni) and 4*f*, 5*d*, 6*s* (Gd) unpaired electrons. The field-reversal asymmetry of the Fe sample is the strongest, while it is slightly weaker for the Co sample, and only a small effect is observed for the Ni and Gd samples. Actually, the experimental results are well-reproduced by the first principles calculation considering polarization of electrons and positrons as shown by the solid lines.

The relative amplitude of the differential DBAR spectra of the Fe, Co and Ni samples seems to coincide with the trend of effective magnetization of these metals. If the area intensity of the Fe sample is normalized to 2.2, those of Co and samples are 1.8 and 0.4. These are comparable to the effective magnetizations of these materials. This result indicates that the magnetization of a magnetic substance can be estimated from the field reversal asymmetry of DBAR spectrum using a reference sample with known magnetization. Considering the fact that the electron polarization of Fe is at most about 40 % near the Fermi level, the determination of electron polarizations of half-metals by the present method is feasible.

In SP-PAS experiment, polarized electrons are directly detected through annihilation with polarized positrons. This is an important feature for the investigation of polarized electron states. The further advantage of SP-PAS is the depth selectivity by employing monochromatic positron beams. Some important magnetic effects, such as giant magnetoresistance and tunneling magnetoresistance, occur near the interface between magnetic and non-magnetic layers. Spin-injection electrodes, which will be used in spin devices, are normally thin films. Novel spin phenomena such as the spin Hall effect and the giant Rashba effect occur near surfaces. These are potential applications of SP-PAS. Taking advantage that PAS is a powerful tool to detect vacancy defects, SP-PAS might be used in studying vacancy-induced magnetism.

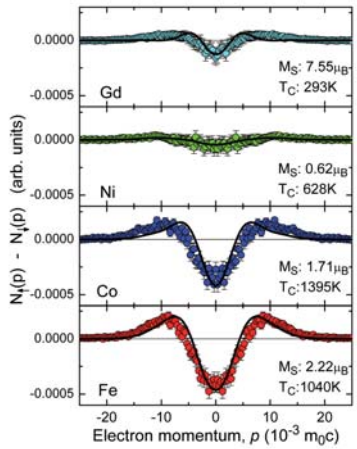

Fig. 1 Differential DBAR spectra of the Fe, Co, Ni and Gd samples obtained in the external magnetic field of 1 T at room temperature. These spectra are folded at p = 0 to enhance the statistics. Solid lines denote calculated differential DBAR spectra. The amplitudes are adjusted to levels comparable with the experiments.

References

[1] S. Berko, *in Positron annihilation*, ed. by A. T. Stewart and L. O. Roelling (Academic Press, New York, 1967), p.61.
[2] A. Kawasuso *et al*., Phys. Rev. B **83**, 100406(R) (2011).

REIMEI Research Project: New approach to the exotic phases of actinide compounds under unconventional experimental conditions

G. H. Lander[1)], A. Hiess[1)], and S. Kambe[2)]
1) ILL 2) R.G. for Condensed Matter Physics of Heavy Element Systems, ASRC, JAEA

We have proposed development of measurements for actinides compounds under unconventional conditions i.e. highly radioactive (transuranium, ^{235}U-enriched) materials, high magnetic field, high pressures on international collaborations of several institutes which have their own special techniques, in order to discover and clarify the exotic electronic properties in 5*f*-electron systems, which appear only under extreme conditions due to large energy scales (Fermi energy, Kondo temperature), compared with 4*f*-systems. A special emphasis is put to combine *in-situ* bulk measurements with scattering methods to gain microscopic insight into the various phases in such systems. Because of the difficulty for international transport of actinides samples, researchers and techniques has been encouraged to travel and collaborate to develop and perform the investigations. We describe below some of the collaborations that have been established in the first year of operating the REIMEI project which continues in 2011-2012. 1) High magnetic field NMR using ^{29}Si-enriched URu_2Si_2 in NHMFL, USA Collaboration between JAEA, LANL and NHMFL underway at NHMFL. 2) Energy scale of the electron-boson spectral function and superconductivity in $NpPd_5Al_2$. Collaboration between ITU and JAEA. Experiments at JAEA with theory at ITU and University of Turin [1]. 3) Search for quadrupolar ordering in the hidden ordered phase of URu_2Si_2. Collaboration between ITU and CEA with experiments at ESRF [2]. 4) Resonant X-ray emission spectroscopy at the L_3 edge of americium up to 23 GPa [3]. Collaboration between ITU and ESRF, with experiments at ESRF. 5) Understanding the complex phase diagram of uranium: the role of electron-phonon coupling. Collaboration between CEA, ITU, and LANL. Experiments at ESRF with theory at CEA. In addition, the first International ASRC Workshop has been held on this subject in Tokai, 16-18 Feb 2011 (photo on the cover page) .The topics 1) and 2) are selected to be described in detail below.

High magnetic field NMR using ^{29}Si-enriched URu_2Si_2 in NHMFL

Several single crystals of URu_2Si_2 enriched to 99.8 at. % by ^{29}Si isotope were shipped from LANL to NHMFL. In this first NMR measurement by JAEA and NHMFL NMR groups, we have characterized the sample quality. The line width of ^{29}Si - NMR at 6.7 T is around 10 kHz for *H*//a, which is quite narrow indicating a good homogeneity of sample. In fact, this line width value is consistent with the previously reported line width in non-enriched sample if we consider some additional line broadening due to the dipolar contribution from ^{29}Si nuclei. In addition, T-dependence of nuclear spin-lattice time has been found to be same as the previously reported value in a high quality non-enriched sample. The ^{29}Si-enrichment can reduce the magnet time very efficiently. For the next measurement in the higher field, we will concentrate to measure the temperature dependence of NMR spectrum under the several higher fields up to 29 T, in order to identify the phase transition around 22 T, which would be accompanied with a change of Fermi-surface.

The energy scale Ω_0 of the electron-boson spectral function in the heavy-fermion, *d*-wave superconductor $NpPd_5Al_2$

This has been predicted on the basis of Eliashberg theory calculations (Fig.1). Assuming a spectral function shape typical for antiferromagnetic spin fluctuations, and imposing constraints provided by the experimental values for the critical temperature and the low-temperature energy gap, one obtains values of Ω_0 of about 2-2.5 meV, slightly dependent on the strength of the Coulomb pseudopotential. These values are in excellent agreement with the characteristic magnetic fluctuations energy estimated from NMR measurements of the nuclear spin-lattice relaxation time at the Al site. The calculated temperature dependence of the upper critical field, the local spin susceptibility, and the nuclear spin-lattice relaxation rate is also in good agreement with available experimental data, showing that a coherent description of the superconducting state can be obtained assuming that the electron pairing in $NpPd_5Al_2$ is mediated by antiferromagnetic fluctuations [1]. Inelastic neutron scattering experiments are planned to confirm the proposed scenario.

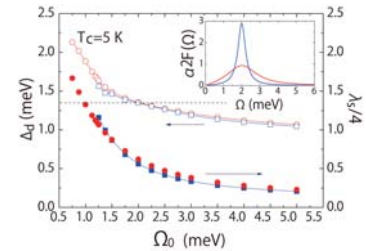

Fig. 1 Gap values Δ_d calculated at T = 0.25 K assuming a Coulomb pseudopotential μ_d^* = 0, and an Eliashberg spectral function centered at an energy Ω_0 and having full width at half maximum of 1 meV (red, open circles) or 0.25 meV (blue, open squares). The horizontal dashed line represents the experimental value of μ_d^*. (Right axis) Electron boson coupling constant λ_s as a function of Ω_0, for Tc = 5 K, μ_d^* = 0, and FWHM of 1 meV (red, closed circles) or 0.25 meV (blue, closed squares). The inset shows the electron-boson spectral function in the two cases.

References

[1] G. A. Ummarino, R. Caciuffo, H. Chudo, and S. Kambe, Phys. Rev. B **82**,104510 (2010).
[2] H. Walker, R. Caciuffo, D. Aoki, F. Bourdarot, G. H. Lander, and J. Flouquet, Phys. Rev. B **83**, 193102 (2011).
[3] S. Heathman, J.-P. Rueff, L. Simonelli, M. A. Denecke, J.-C. Griveau, R. Caciuffo, and G. H. Lander, Phys. Rev. B **82**, 201103R (2010).

Research Group for Condensed Matter Theory

Group Leader: Michiyasu Mori

Electric power generation and storage are indispensable for our lives. Although the nuclear power plant produces a huge amount of energy, the most part is dissipated away by the heat flow. To enhance its efficiency, the thermoelectric material is one of plausible candidates. We study such functional materials emerging from the electrons internal degrees of freedom (spin, charge and orbital) by combining various numerical methods and quantum field theory. Our results on spin Seebeck effect and giant spin-Hall effect must play a role to develop new thermoelectric material and device.

Theory of spin Seebeck effect in ferromagnetic insulators

Electric power generation by a temperature gradient (Seebeck effect) is one of important issues in condensed matter physics, since such a thermoelectric device possesses several appealing features necessary for future technologies. However, most of thermoelectric devices adopt conductors, and thereby its low efficiency due to the energy loss by conduction electrons scattering prevents the thermoelectric devices from practical applications.

Using a prototypical magnet ($LaY_2Fe_5O_{12}$), Saitoh and co-workers experimentally established a new principle that spin-current generation by a temperature gradient, so-called spin Seebeck effect, occurs in an insulating magnet even in the absence of conduction electrons [1] (See Fig.1). They established another principle that a spin current flowing in a magnetic insulator can be converted into the electricity [2]. By these two principles, the insulator-based thermoelectric devices can be realized. Electric voltage generation from heat flow in an insulator is a new principle of thermoelectric device, and has never been considered so far.

We investigate a gigantic enhancement of the spin Seebeck effect in a prototypical magnet $LaY_2Fe_5O_{12}$ at low temperatures [3]. Our theoretical analysis sheds light on the important role of phonons; the spin Seebeck effect is enormously enhanced by nonequilibrium phonons that drag the low-lying spin excitations. We further argue that this scenario gives a clue to understand the observation of the spin Seebeck effect that is unaccompanied by a global spin current, and predict that the substrate condition affects the observed signal.

In addition, we formulate a linear response theory of the spin Seebeck effect [4]. Our approach focuses on the collective magnetic excitation of spins, i.e., magnons. We show that the linear-response formulation provides us with a qualitative as well as quantitative understanding of the spin Seebeck effect observed in the magnetic insulator.

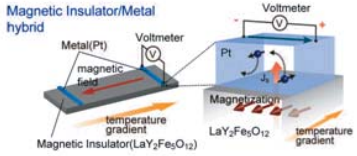

Fig. 1 Spin Seebeck effect in the magnetic insulator ($LaY_2Fe_5O_{12}$).

Giant spin Hall effect (SHE) of Au films with Pt impurities

The SHE indispensable for the spin-electronics and the spin Seebeck effect is induced by the spin-orbit interaction (SOI). We study the SOI of an Fe impurity in Au host metal by quantum Monte Carlo (QMC) simulation of a realistic multiorbital Anderson impurity model [5]. We show that the SOI is strongly renormalized by the quantum spin fluctuation. Based on this mechanism, we can explain why the gigantic SHE in Au with Fe impurities was observed in recent experiments, while it is not visible in the anomalous Hall effect. In addition, we show that the SOI is strongly renormalized by the Coulomb correlation U. Based on this picture, we can explain past discrepancies in the calculated orbital angular momenta for an Fe impurity in an Au host.

In addition, we show theoretically a novel route to obtain giant room temperature SHE using surface-assisted skew scattering [6,7]. By a combined approach of density functional theory and the QMC method, we have studied the SHE due to a Pt impurity in different Au hosts. We show that the spin Hall angle could become larger than 0.1 on the Au (111) surface, and decreases by about a half on the Au (001) surface, while it is small in bulk Au. The QMC results show that the SOI of the Pt impurity on the Au (001) and Au (111) surfaces is enhanced, because the Pt 5d levels are lifted to the Fermi level due to the valence fluctuations. In addition, there are two SOI channels on the Au (111) surface, while only one for Pt either on the Au (001) surface or in bulk Au.

Enhanced pairing correlations near oxygen dopants in cuprate superconduct

Recent experiments on Bi-based cuprate superconductors have revealed an unexpected enhancement of the pairing correlations near the interstitial oxygen dopant ions. In this study, we propose a possible mechanism -- based on local screening effects -- by which the oxygen dopants do modify the electronic parameters within the CuO_2 planes and strongly increase the superexchange coupling J [8]. This enhances the spin pairing effects locally and may explain the observed spatial variations of the density of states and the pairing gap. The effect is of an entirely dynamical nature and thus goes beyond the band structure calculations. Apart from the STM experiments, there is an interesting possibility to test our theory by the resonant inelastic x-ray scattering; it monitors the high-energy spin excitations, and a broad distribution of J values predicted here can be directly observed.

References

[1] K. Uchida *et al.*, Nature Materials **9**, 894 (2010).
[2] Y. Kajiwara *et al.*, Nature **464**, 262 (2010).
[3] H. Adachi *et al.*, Appl. Phys. Lett. **97**, 252506 (2010).
[4] H. Adachi *et al.*, Phys. Rev. B **83**, 094410 (2011).
[5] B. Gu *et al.*, Phys. Rev. Lett. **105**, 086401 (2010).
[6] B. Gu *et al.*, Phys. Rev. Lett. **105**, 216401 (2010).
[7] B. Gu *et al.*, J. Appl. Phys. **109**, 07C502 (2011).
[8] G. Khaliullin *et al.*, Phys. Rev. Lett. **105**, 257005 (2010).

Research Group for Molecular Spintronics

Group Leader: Seiji Sakai

Spintronics is an emerging technology taking advantage of the dual freedom of both charge and spin degrees. Since the discovery of the giant magnetoresistance effect in 1988, spintronics has been developed based on inorganic substances like metals and semiconductors. Recent studies have started to shed light on the spintronic application of organic molecules (OMs) and nanocarbons (NCs), in which the spins of conduction electrons can be preserved for a long time and distance. We call this new field "Molecular spintroncis". In molecular spintronics, the efficient control of the spin transport process (e.g., spin-injection, modulation, detection and accumulation) in OMs and NCs by using magnetic heterostructures is of special importance to realize spintronic applications taking advantages of the potential for spin transport media. Our group aims at establishing the advantages of OMs and NCs as innovative spintronic materials by developing novel systems for spin operations based on the hybrid structures of OMs/NCs and magnetic transition metals and by employing advanced spectroscopic techniques on the electronic and spin structures in such systems.

Finding of difference in interactions with ferromagnetic metals between single-layer and multilayer graphene

Understanding chemical interactions and electronic structures at the graphene/magnetic metal interfaces is of special importance in designing spin opeartion sources for graphene-based spintronic devices. The influence of the interface formation with ferromagnetic metals on the vibrational properties of graphene was investigated by using confocal micro-Raman spectroscopy [1,2]. Micro-Raman measurements on the micrometer-scale patterned graphene/ferromagnetic metal heterostructures [Fig. 1(a)], which are consisting of patterned regions of the graphenes with various layers number covered with and without metals on the same graphene sheet, enables us to examine the interactions at the graphene/ferromagnetic metal interface as a function of the graphene layers number. From the dependences of the peaks shifts of the Raman bands (e.g., the G band) on the graphene layers number [Fig. 1(b)], it is revealed that the interfacial interactions with ferromagnetic metal are dramatically different between single-layer graphene (SLG) and multilayer graphene (MLG): In the MLG/ferromagnetic metal heterostructures, the Raman bands show a gradual shift in the peak position depdending on the layers number, which are reasonably attributed to electron doping from the ferromagnetic metal to a few graphene layers from the interfaces. Meanwhile, the SLG/ferromagnetic metal heterostructures show a different band-shift feature as in Fig.1, suggesting that there exist strong covalent interactions between SLG and the ferromagnetic metal. The present study would provide important information for improving the performance (e.g., the spin-injection efficiency and interfacial resistance) of graphene-based spintronic devices.

Elucidation of very high spin polarization at fullerene-transition metal compound/ferromagnetic metal interface

The tunneling magnetoresistance (TMR) effect of granular fullerene-cobalt (C_{60}-Co) films [3-5] was studied in the current-perpendicular-to-plane geometry to elucidate the spin-dependent tunneling process bringing about a remarkably high magnetoresistance as compared to the expectations from the conventional theory. The occurrence of cooperative tunneling (so-called cotunneling) through a few to several Co nanoparticles is confirmed from the current-voltage characteristics in the Coulomb blockade regime. Analysis based on the cotunneling model considering the magnitudes of the zero-bias magnetoresistance ratios ($\Delta R/R_{max}$ = 90% at low temperatures) reveals that the spin polarization (P) of tunneling electrons generated at the C_{60}-Co compound/Co interface is remarkably high (P = 80%) compared to that in Co crystal (P = 37%). The present study suggests that the spin polarization of conduction electrons can be tuned with a proper design of the OM-/NC-transition metal hybrid structures, unlimited by the spin polarization in ferromagnetic metals and also overcoming the problems of interfacial degradation.

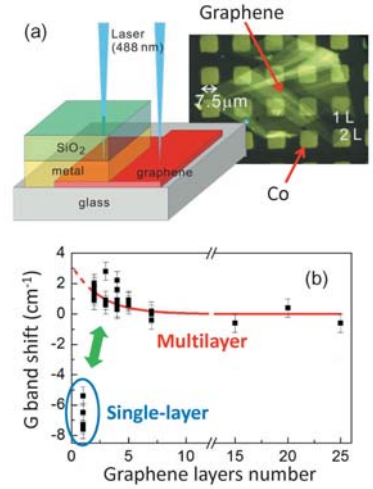

Fig. 1 (a) Schematic drawing and optical image of the micro-patterned graphene/Co sample with the SiO_2/Co/graphene/glass layer structure in the bright areas. The graphene sheet contains more than ten regions with various layers numbers (L) (e.g., 1 L, 2 L), as can be seen from the color. (b) Graphene layers number dependence of the G band shift induced by the heterostructure formation with Co.

References

[1] S. Entani *et al.*, J. Phys. Chem. C **114**, 20042 (2010).
[2] S. Entani *et al.*, Jpn. J. Appl. Phys. **50**, 04DN03 (2011).
[3] S. Sakai *et al.*, Appl. Phys. Lett. **89**, 113118 (2006).
[4] S. Sakai *et al.*, Appl. Phys. Lett. **91**, 242104 (2007).
[5] I. Sugai *et al.*, J. Appl. Phys. **108**, 063920 (2010).

Research Group for Mechanical Cotrol of Materials and Spin Systems

Group Leader: Eiji Saitoh

The research objectives of Spin Manipulation and Material Design Research Group are to develop new methods for controlling spin currents by combining electron spins and mechanical rotation, and/or by coupling spins and NMR techniques;

1) Magnetization manipulation in terms of mechanical rotation.

2) Detection of a spin current generated from rotating objects using the spin-Hall and spin torque effect.

3) Detection of the coupling between nuclear spin and electron spin dynamics and/or current.

Utilizing the combination between spin and mechanical rotation will help us realize an actuator driven by a spin current in a nano scale and mechanical generator of spin currents.

Construction of experimental setups for spin manipulation by high-speed rotation and NMR technique

To control the spin current with the new methods, we newly constructed two experimental setups, one was a high-speed rotator, and the other was a NMR spectrometer. Figure 1 shows a schematic diagram and the constructed apparatus for magnetization manipulation experiments by high-speed rotation.

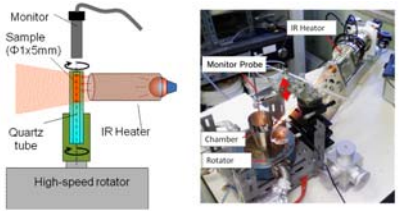

Fig. 1 A schematic diagram and the constructed experimental setup for magnetization manipulation experiments by high-speed rotation.

Spin pumping efficiency of half metalic Co_2MnSi

In the field of spintronics, the methods of generating a pure spin current are important techniques to drive devices such as spin-based magnetic memorites and computing devices. Spin pumping is a recently developed technique to generate a pure spin current. Efficiency of the spin pumping is determined by a spin mixing conductunce, that depends on a difference in the population between up and down spins. Thus half metallic compounds, which have perfectly spin-polarized conduction electrons because of a semi-conducting gap in either the up- and down-spin channel at the Fermi level, are expected to show a high efficiency of the spin pumping. We evaluated the efficency of the spin pumping from a half-metallic Heusler alloy Co_2MnSi film using a ferromagnetic resonace (FMR) technique.

The sample is a Co_2MnSi/Pt bilayer film comprising a 20-nm-thick ferromagnet Co_2MnSi and a 7-nm-thick paramagnet Pt layer as illustrated in Fig. 2. The (100)-oriented epitaxial Co_2MnSi was grown on a MgO(100) substrate with the 0.5-mm thickness by a ultra high vacuum (UHV) sputtering system at ambient temperature, then annealed at 723 K to improve crystal quality and chemical ordering. The sample system is mounted on the center of a TE_{011} microwave cavity, where the magnetic field component of the microwave mode $\boldsymbol{h}_1$ is maximized. The frequency of microwave is 9.44 GHz.

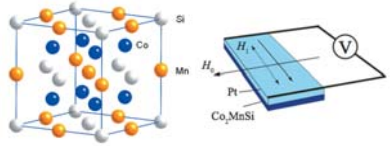

Fig. 2 A crystal structure of Co_2MnSi and a schematic illustration of the sample.

The upper panel of Fig. 3 shows the field swept FMR spectrum dI/dH and the lower one shows the field dependence of the potential difference between electrodes on the Pt film, respectively. At the center of resonance, a spin current generated by FMR in the Co_2MnSi layer is injected into the Pt layer. The pure spin current injected into the Pt layer from the Co_2MnSi layer is detected by the inverse spin-Hall effect (ISHE), which converts the spin current into an electric current. We estimated a damping constant of the Co_2MnSi/Pt bilayer film from an angular dependence of FMR spectra. Analyzing the damping constant efficiency of the spin pumping from the Co_2MnSi layer is evaluated. We found that a mixing conductance at the Co_2MnSi/Pt interface is comparable to that at a permalloy/Pt interface.

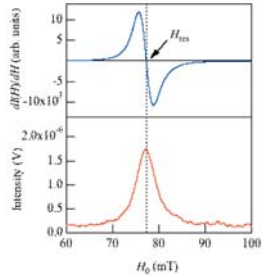

Fig. 3 The upper panel shows field dependence of the FMR signal dI = dH for a Co_2MnSi/Pt bilayer film, where I denotes the microwave absorption intensity, and the lower shows field dependence of the potential difference between electrodes on the Pt film. The dotted line in the panel represent the resonant field of 772.6 Oe.

Reference

[1] H. Chudo *et al.*, J. Appl. Phys. **109**, 073915 (2011).

Research Group for Reactions Involving Heavy Nuclei

Group Leader: Satoshi Chiba

The objectives of Research Group for Reactions Involving Heavy Nuclei are to develop experimental and theoretical methods to realize and validate the surrogate reaction technique to determine neutron-induced reaction cross sections of unstable nuclei such as minor actinides and branch-point nuclei of s-process nucleosynthesis. We specialise to surrogate reactions using heavy projectiles. Experimental apparatus to measure fission and capture cross sections were developed and installed at Tandem accelerator facility as shown in Fig. 1. At the same time, basic researches in related areas, especially, shell structure and reaction characteriscis of (heavy, fissionable) nuclei are also in our important scope. These results are published as a number of papers. Highlights of our activities during FY 2010 are summarized below.

Nuclear orientation in the reaction ^{34}S+^{238}U and synthesis of the new isotope ^{268}Hs

The synthesis of isotopes of the element hassium was studied using the reaction $^{34}S + {}^{238}U \rightarrow {}^{272}Hs^*$ [1]. At a kinetic energy of 152.0 MeV in the center-of-mass system one decay of the new isotope ^{268}Hs was observed. It decays with a half-life of $0.38^{+1.8}_{-0.17}$ s by 9479±16 keV α-particle emission. Spontaneous fission of the daughter nucleus ^{264}Sg was confirmed. The measured cross section was $0.54^{+1.3}_{-0.45}$ pb. The fission-fragment mass distributions changed from symmetry to asymmetry when the beam energy was changed from above-barrier to sub-barrier values, indicating orientation effects on fusion and/or quasifission. It was found that the distribution of symmetric mass fragments originates not only from fusion-fission, but has a strong component from quasifission. The result was supported by a calculation based on a dynamical description using the Langevin equation, in which the mass distributions for fusion-fission and quasifission fragments were separately determined.

In-beam γ-ray spectroscopy of ^{248,250,252}Cf by neutron-transfer reactions using a Cf target

The ground-state bands of ^{248}Cf, ^{250}Cf and ^{252}Cf have been established up to the 10^+, 12^+, and 10^+ states, respectively, by in-beam γ-ray spectroscopy using neutron-transfer reactions with a 153-MeV ^{18}O beam and a highly radioactive Cf target [2]. The deexcitation γ rays in ^{248}Cf, ^{250}Cf and ^{252}Cf were identified by taking coincidences with outgoing particles of $^{16-19}$O measured with Si ΔE-E detectors, and by selecting their kinetic energies. Moments of inertia of ^{248}Cf, ^{250}Cf and ^{252}Cf were discussed in terms of the $N = 152$ deformed shell gap.

Theoretical investigation of the surrogate reaction method

Results of the surrogate reactions depend sensitively on the difference of populated spin distribution from that of desired neutron-induced reactions. The spin distribution, in turn, reflects reaction mechanisms and underlying nuclear structure. We therefore try to find a universal condition that surrogate reactions would yield the desired neutron cross sections. For this aim we discussed the surrogate ratio method, and it was found that we need not know the spin-parity distributions populated by surrogate reaction, if (1) there exist two surrogate reactions whose spin-parity distributions of decaying nuclei are almost equivalent, and (2) difference of representative spin values between the neutron-induced and surrogate reactions is not much larger than 10$\hbar$, and (3) J^{π}-by-J^{π} convergence of the decay branching ratio is achieved (which can be verified by a statistical model) [3]. Successive theoretical works followed to confirm this conclusion. Experimental equipments were designed accoring to the above considerations.

To understand the reaction mechanism and verify the above conditions for the surrogate ratio method to work, we established a theoretical model which is based on the unified model. We performed a trajectory calculation on the time-dependent unified potential energy surface using the Langevin equation. Using the model, we calculated the spin of the compound nucleus in surrogate reactions ^{236,238}U(^{18}O, ^{16}O)^{238,240}U. The results show the spin of compound nucleus is less than 10$\hbar$ (namely, condition (2) is satisfied). We also calculated the spin distributions of decaying nuclei by these two reactions, and found that they were indeed equivalent (condition (1) is satisfied). The present results suggested the validity of the surrogate ratio method.

In approaching the surrogate reaction from the viewpoint of full quantum mechanics, nuclear-structure information on the projectile and target nuclei is strongly desired. We thus calculated the structure of oxygen isotopes with the shell model in the full *p-sd* valence space [4] because ^{16}O beam is used in our surrogate reactions. Since in previous microscopic calculations some low-lying states, known as multiparticle-multihole states excited across the $N = Z = 8$ shell gap, were too high compared with experimental data, we focused on the mechanism that lowers these states. It turned out that due to large correlation energy in ^{16}O the $N = Z = 8$ shell gap must be strongly reduced from the standard value which is based on the assumption of a closed shell for ^{16}O. This reduction plays a key role in accounting for the lowering of the multiparticle-multihole states.

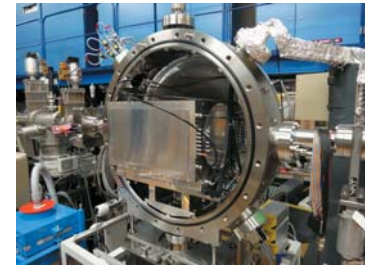

Fig. 1 Vacuum chamber and MWPC (multi-wire proportional counter) installed at Tandem accelerator facility in Tokai.

References

[1] K. Nishio *et al.*, Phys. Rev. C. **82**, 024611 (2010).
[2] R. Takahashi *et al.*, Phys. Rev. C. **81**, 057303 (2010).
[3] S. Chiba and O. Iwamoto, Phys. Rev. C **81**, 044604 (2010).
[4] Y. Utsuno and S. Chiba, Phys. Rev. C **83**, 021301(R) (2011).

Research Group for Superheavy Elements

Group Leader: Matthias Schädel

The research objectives of this group are to understand chemical and nuclear properties of superheavy elements (SHEs) placed at the uppermost end of the Periodic Table and on the heaviest frontier of the nuclear chart. To clarify chemical properties of SHEs, we investigate valence electronic structures of SHEs through experimental determinations of ionic radii, redox potentials, ionization potentials, and formation of chemical compounds of SHEs. To elucidate limits of stability of the heaviest nuclei, we investigate the shell structure of superheavy nuclei through experimental assignments of proton and neutron single-particle orbitals and through the evolution of nuclear deformation at the highest proton and neutron numbers. Research topics in this fiscal year are summarized below.

Chemical properties of element 104, rutherfordium (Rf), in HCl solution: extraction chromatography using TOPO

From a simple extension of the Periodic Table of the Elements, element 104, Rf, should be a transition element and belong into group 4. Although chemical properties of Rf are expected to be similar to those of lighter homologues Zr and Hf, some significant differences are found in HCl and HF solutions [1–3], which provides valuable information on the valence electronic structure of Rf. In the present work, the extraction behavior of Rf onto a styrenedivinylbenzene copolymer resin modified by trioctylphosphine oxide (TOPO) from 2.0–7.0 M HCl solutions was investigated together with Zr and Hf [4]. TOPO has a chemical structure similar to that of tributylphosphate (TBP) and has a higher basicity value as a donor than that of TBP. The effect of the basicity of organophosphorus compounds on the strength of the formation of a Rf complex was examined by comparing the extraction sequence of the group-4 elements into TOPO with that into TBP [2]. The extraction yields of Rf, Zr, and Hf increased with an increase of HCl concentration, and the sequence of their extraction was Zr > Hf ≥ Rf as shown in Fig. 1. The result indicates that the stability of the $RfCl_4$·2(TOPO) complex is lower than that of the corresponding species of Zr and Hf. A basicity effect in the formation of TOPO and TBP complexes was not observed in the extraction sequence among Rf, Zr, and Hf in HCl solution.

First detailed spectroscopy for short-lived heavy actinide nuclei: the α decay of ^{255}No

Excited states in ^{251}Fm populated via the α decay of ^{255}No were studied in detail through α-γ coincidence and α fine-structure measurements [5]. Spin-parities and neutron single-particle configurations of the excited states in ^{251}Fm as well as the ground state of ^{255}No were unambiguously identified on the basis of deduced internal conversion coefficients, lifetimes of γ transitions, rotational-band energies built on one-quasiparticle states, and hindrance factors of α transitions. In particular, the α fine-structure spectrum (shown in Fig. 2) enabled us to firmly establish neutron one-quasiparticle states in ^{251}Fm and their rotational-band structures. Figure 3 shows excitation energies of neutron one-quasiparticle states in N = 151 isotones. It was found that the energy of the 1/2$^+$[620] state in the N = 151 isotones increases with the atomic number, especially at $Z \geq 100$ (^{251}Fm). This indicates that the N = 152 deformed shell gap size becomes larger as the atomic number increases. We calculated ground-state deformations and energies of one-quasiparticle states in the N = 151 isotones using a macroscopic-microscopic model, and found that the evolution of nuclear deformation involving the hexadecapole (β_4) and hexacontatetrapole (β_6) deformations largely contributes to the single-particle structures in the $Z \geq 100$ and $N \geq 152$ nuclei.

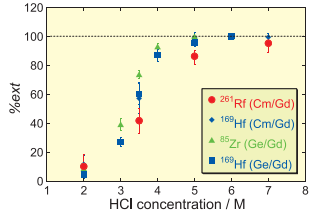

Fig. 1 Extraction of Rf, Zr, and Hf on 0.04 M TOPO as a function of HCl concentration. Cm/Gd and Ge/Gd represent targets used for the production of ^{261}Rf, ^{169}Hf, and ^{85}Zr.

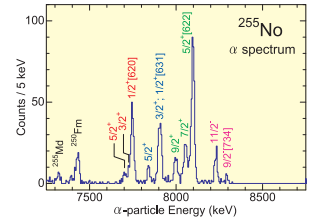

Fig. 2 α -energy spectrum of ^{255}No.

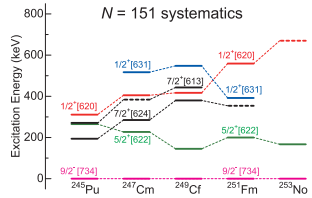

Fig. 3 Excitation energies of neutron one-quasiparticle states in N = 151 isotones.

References

[1] H. Haba *et al.*, J. Nucl. Radiochem. Sci. **3**, 143 (2002).
[2] H. Haba *et al.*, Radiochim. Acta **95**, 1 (2007).
[3] A. Toyoshima *et al.*, Radiochim. Acta **96**, 125 (2008).
[4] A. Toyoshima *et al.*, J. Nucl. Radiochem. Sci. **11**, 7 (2010).
[5] M. Asai *et al.*, Phys. Rev. C **83**, 014315 (2011).

Research Group for Actinide Materials Science

Group Leader: Zachary Fisk

Many important properties of actinide elements and their compounds are determined by their 5*f* electrons. Because of the large number of degrees of freedom of 5*f* electrons and their sensitivity to chemical/physical environment, a variety of phenomena are realized. In a new compound an actinide experiences a different ligand field, with strong physical effects. Pressure modifies the interatomic distance continuously and this in turn has immediate influence on the 5*f* electronic behavior. Finally the purification of a known compound also provides us a new insight particularly for phenomena occurring at low temperatures, where impurity disorder can deeply disturb and hence hide the intrinsic behavior. Our group uses various techniques for the crystal growth and characterization of actinide compounds including highly radioactive transuranium elements. Hydrostatic pressure will be used to modify the electronic state by tuning the interatomic distances.

Ultra clean sample of URu_2Si_2 and the hidden order

URu_2Si_2 is a uranium-based intermetallic compound crystallizing in a tetragonal crystal structure (Fig. 1). It has two phase transitions. One is the superconducting transition at 1.4 K. Another one occurring at 17.5 K accompanies a thermodynamic anomaly. However the order parameter of the latter one is still unknown despite the huge experimental effort since its discovery in 1985. Using a high-quality single crystal with a very low residual resistivity from impurity scattering, new features were found by utilising novel experimental techniques.

Photoemission spectroscopy is a powerful tool to observe electronic band structure. By using a recently developed high energy-resolution laser photoemission, it was found that a narrow quasiparticle band appears below the hidden-order transition temperature [1]. On the other hand, a cantilever magnetometer measurement succeeded to detect a symmetry-breaking in the hidden order state. The four-fold anisotropy expected for the tetragonal basal plane is changed to the two-fold (orthorhombic) symmetry below the hidden-order transition temperature [2]. These observations provide new insights to the nature of the hidden-order state and accelerate further experimental and theoretical investigations. See 'Research Highlights' for details.

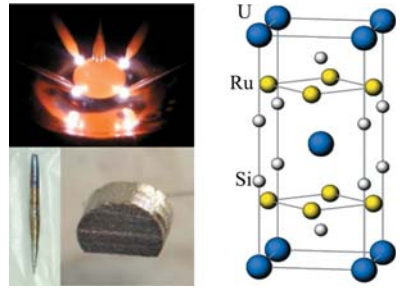

Fig. 1 (left) Czochralski-pulling method and a single crystal of high-quality URu_2Si_2. (right) Tetragonal crystal structure of URu_2Si_2.

Defect structure analysis of fluorite-based solid solutions

A variety of fluorite-based solid solutions are formed between $M^{4+}O_2$ (M = Ce, Th) and $Ln^{3+}{}_2O_3$ (Ln = lanthanide). The lattice parameter data of these $M_{1-y}Ln_yO_{2-y/2}$ solutions exhibit marked deviation from the Vegard's law (i.e., the linear variation with the Ln concentration y), most plausibly originating from the formation of oxygen vacancy (V_o) in the anion sublattice. However, this V_o effect has been neither well recognized nor well modeled. We carefully analysed the lattice parameter data, one of the most fundamental macroscopic quantity, of the solutions, and clarified their 'generalized non-Vegardian' behavior with non-random oxygen coordination around the cations. The present model is thus found to be useful not only as a new quantitative lattice-parameter model but also as a new direct-link to their controversial non-random local defect structure. For example, this can provide a new consistent description of their intriguing ionic-conductivity maxima behavior in low y range [3,4].

Hydrostatic pressure technique for actinide study

High pressure technique is a very useful tool to modify electronic states of actnide compound. Since the properties of actinide compounds are sensitive to the pressure inhomogeniety or uniaxial stress occurring at low temperature, it is necessary to achieve hydrostatic conditions. We have built a diamond anvil cell and selected appropriate pressure medium for the low-temperature and high-pressure experiments up to 10 GPa with nearly hydrostatic conditions [5].

The pressure technique was applied to the uranium-based antiferromagnet U_2Zn_{17} [6]. In general, application of pressure on localized cerium antiferromagnet suppresses the transition temperature at high pressure and drives the system to non-magnetic heavy electron state because of competing two effects, antiferromagnetic exchange and the Kondo interactions. In U_2Zn_{17}, however, the antiferromagnetic transition temperature is almost unchanged up to 5 GPa and gradually increasing above 5 GPa up to 9 GPa. Higher pressure far above 10 GPa is necessary to suppress the transition temperature, in contrast to the typical critical pressure of 2 GPa for the cerium compound with the similar bulk modulus. The weak pressure effect may be ascribed to the itinerant character of 5*f* electrons in this compound, as discussed theoretically in uranium monochalcogenide.

References

[1] R. Yoshida *et al.*, Phys. Rev. B **82**, 205108 (2010).
[2] R. Okazaki *et al.*, Science **331**, 439 (2011).
[3] A. Nakamura, Solid State Ionics **181**, 1543 (2010).
[4] A. Nakamura, Solid State Ionics **181**, 1631 (2010).
[5] N. Tateiwa *et al.*, J. Phys.: Conf. Ser. **215**, 012178 (2010).
[6] N. Tateiwa *et al.*, J. Phys. Soc. Jpn. **80**, 014706 (2011).

Research Group for Condensed Matter Physics of Heavy Elements Systems

Group Leader: Shinsaku Kambe

In heavy element (*f*-electron) systems, valence fluctuations, the Kondo effect, and the RKKY interaction compete with one another. Because of this, exotic behaviors such as quantum critical points, heavy fermions, non-Fermi liquids, anisotropic superconductivity and multipolar ordering appear when such competition is strong. Recently, it has become clear that these exotic behaviors for 5*f*-electron systems are different from those for 4*f*-electrons. This is because electrons with different spin and orbital character can coexist in 5*f* actinide systems, in contrast to the case of 4*f*-electrons. By means of microscopic spectroscopy: NMR and μSR, our research group tries to clarify these exotic behaviors due to the "many-fold" character of 4*f*, 5*f* compounds, including transuranium. 5*f*-electron systems are regarded to possess intermediate physical properties between those of 3*d*- and 4*f*-electrons systems. The final scientific goal of our project is to unify the concept of magnetism and superconductivity for 3*d* through 5*f* systems.

Correlation between the superconducting pairing symmetry and magnetic anisotropy in *f*-electron unconventional superconductors

The superconducting pairing symmetry and the magnetic anisotropy of the normal state are found empirically to be strongly correlated in *f*-electron unconventional superconductors having crystallographic symmetry lower than cubic [1]. Effectively, there are three categories: 1)In antiferromagnetic systems, unconventional superconductivity appears with singlet (*d*-wave) pairing or mixed-parity pairing (in non-centrosymmetric compounds) for cases of XY anisotropy. 2) In ferromagnetic systems, unconventional superconductivity with triplet (e.g. *p*-wave) pairing appears for cases of Ising anisotropy. 3) A few exceptional cases: The origin of the observed correlation is discussed in terms of the orbital *f*-electron states. Especially, in the case 1), the larger magnetic XY anisotropy would produce the higher-T_c *d*-wave superconductivity [2].

Microscopic evidence for magnetic transition in AmO_2

The first NMR study of americium dioxide (AmO_2) has been done. More than 30 years ago, a phase transition was suggested to occur in this compound at 8.5 K based on magnetic susceptibility data, while no evidence had been obtained from microscopic measurements. We have prepared a powder sample of $^{243}AmO_2$ containing 90 at. % ^{17}O and have performed ^{17}O-NMR at temperatures ranging from 1.5 to 200 K. After a sudden drop of the ^{17}O NMR signal intensity below 8.5 K, at 1.5 K we have observed an extremely broad spectrum covering a range of ~14 kOe in applied field (Fig. 1). These data provide the first microscopic evidence for a phase transition as a bulk property in this system [3]. In addition, the ^{17}O NMR spectrum has been found to split into two peaks in the paramagnetic state, which has not been reported for actinide dioxides studied up to now. We suggest that the splitting is induced by self-radiation damage from the alpha decay of ^{243}Am.

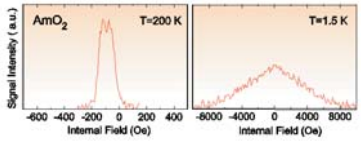

Fig. 1 Temperature dependence of ^{17}O-NMR spectra observed in AmO_2. The shape of the spectrum corresponds to the distribution of hyperfine fields at oxygen nuclear sites. The spectrum in AmO_2 broadens drastically below the ordering temperature of 8.5 K. The line shape in the ordered state is found to be quite different from the rectangular shape observed in the dipole ordered state of UO_2.

***f*-electron anisotropy locally induced by an interstitial hydrogen analogue μ^+ in $PrPb_3$**

There is growing interest in the microscopic knowledge of an interstitial hydrogen in condensed matter and its influence on neighbors. We investigated a microscopic state of the interstitial hydrogen in $PrPb_3$ that is related to lanthanide-based hydrogen absorption metals using a positive muon μ^+ as a hydrogen analogue. We found that the implanted μ^+ is localized at the midpoint between two Pr ions and forms a three spin system Pr-μ^+-Pr, which is evidenced from the time-evolution of μ^+ spin polarization (Fig. 2) [4,5]. The coupling between a ^{141}Pr nuclear spin and a μ^+ spin is anisotropically enhanced by hyperfine-enhanced *f*-electron magnetic moment. This indicates that the interstitial hydrogen locally induces the strong anisotropy in *f*-electron magnetism. Based on this study, the effective crystal field at the Pr site in metallic $PrPb_3$ is clarified.

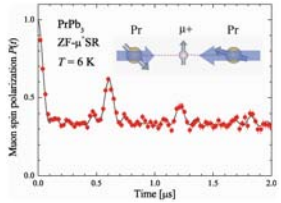

Fig. 2 Time-evolution of μ^+ spin polarization in $PrPb_3$. Characteristic periodic peaks appears due to the formation of Pr-μ^+-Pr system (Inset). The blue arrows represent *f*-electron magnetic moments induced by the hyperfine interaction with Pr nuclear spins.

References

[1] S. Kambe *et al*., J. Phys.: Conf. Ser. (2011) appears on Web.
[2] S. H. Baek, H. Sakai *et al*., Phys. Rev. Lett. **105**, 217002 (2010).
[3] Y. Tokunaga *et al*., J. Phys. Soc. Jpn. **79**, 053705 (2010).
[4] T. U. Ito *et al*., J. Phys.: Conf. Ser. **225**, 012021 (2010).
[5] T. U. Ito *et al*., Phys. Rev. Lett. **102**, 96403 (2009).

Research Group for Hadron Physics

Group Leader: Kenichi Imai

The research objectives of Research Group for Hadron Physics are 1) experimental study of exotic hadrons and nuclei with strangeness and charm at J-PARC and BNL-RHIC, 2) research and development of new high-rate particle detectors such as a silicon strip detector, a scintillation fiber tracker and a time projection chamber, 3) theoretical study of nuclear matter at high and low densities and the role of strangeness in nuclear matter and neutron stars. Through these topics, we study many-body problems of quarks and hadrons in relation with QCD.

Search for penta-quark Θ^+ with a π beam at J-PARC

The experiment to search for the penta-quark Θ^+ has been performed at J-PARC, through $\pi^- p \rightarrow K^- X(\Theta^+)$ reaction. This was the first experiment in the Hadron hall at J-PARC. The J-PARC hadron beam line (K1.8) provides a π^- beam of 1.9 GeV/*c* and 10^6 π^-/spill which hits a liquid hydrogen target. Momentum of π^- beam particles is measured by a beam-line spectrometer and that of outgoing K^- mesons is measured with a kaon spectrometer (SKS). The missing-mass resolution for Θ^+ was expected to be about 1.4 MeV/c^2 which is the best resolution among previous penta-quark search experiments. This missing-mass resolution was confirmed by measuring Σ^- hyperons by $\pi^- p \rightarrow K^+ \Sigma^-$ reaction. The data was analyzed in a short period and we found no peak structure due to Θ^+ in the obtained missing-mass spectrum [1]. It concluded that a hint of a possible peak for Θ^+ at 1.53 GeV/c^2 observed by the previous KEK experiment (E522) was due to a statistical fluctuation, since the present data has 10 times more sensitivity to Θ^+ than the previous experiment. The null result provided an upper limit for the production cross section of Θ^+ to be 150 nb at 90% confidence level. It suggests the width of Θ^+ is expected to be about 100 keV or less if it exists, which is quite different from the known hadron resonances.

Research and development (R&D) of high-rate particle detectors for hadron physics experiments at J-PARC

We have been developing three kinds of detectors which have very high rate capabilities. It is quite important and essential to fully utilize the high intensity hadron beams provided by J-PARC. The goal of this R&D is to install tracking detectors capable up to the rate of 10^8 particles/s, which is 100 times higher than the capability of the present detectors at the beam line at J-PARC. The first one is a silicon microstrip detector. We have constructed a silicon strip sensor of 80 μm strip width and sensitive area of 60 $\times$60 mm^2. A test experiment was performed at the Research Center for Electron Photon Science, Tohoku University using a high-intensity electron beam up to more than 10^7 particles/s. We found this detector has a sufficient efficiency (95%) up to 100 MHz particle rate. The second is a time projection chamber (TPC) which is capable of the three-dimensional track reconstruction. We have constructed a small TPC for R&D which has about 25 cm drift length and 10$\times$10 cm^2 sensitive area. In order to have a high rate capability, gas electron multiplier (GEM) sheets with anode pads are employed for the signal amplification and readout. The third one is a scintillating fiber tracker. It has a high rate capability up to 100 MHz particle rates because of an excellent time resolution (less than 1 ns). The construction of a fiber tracker with 1mm ϕ scintillating fibers with micro pixel photon counter (MPPC) readout is now in progress.

Theoretical study of nuclear matter

The equation of state (EOS) of nuclear matter during the liquid-gas (LG) phase transition is one of the most important issues in nuclear physics and astrophysics. In the collapsing stage of supernovae and the crust region of neutron stars, low-density and inhomogeneous nuclear matter is expected. The EOS of mixed phase is often obtained by simply applying the Maxwell construction or more carefully by solving the Gibbs conditions. The Maxwell construction can be used in the case of *congruent* transition: the coexisting two phases have the same chemical component with different densities. However, nuclear matter which consists of proton, neutron and electron, generally becomes *non-congruent* and the particle fractions take different values in coexisting phases. The Gibbs conditions then give EOS different from that of the Maxwell construction.

In the viewpoint of the congruence, we have clarified properties of symmetric and asymmetric nuclear matter. Without considering the geometrical structures, symmetric nuclear matter behaves *congruently* due to the strong symmetry potential. Therefore the Maxwell construction is applicable. Asymmetric nuclear matter, on the other hand, is *non-congruent* and the Maxwell construction does not work.

Subsequently we have explored LG mixed phase with geometrical structures called nuclear "pasta". We have clarified the effects of the surface tension and the Coulomb repulsion on the "pasta" structures. These finite-size effects restrict the appearance of mixed phase with "pasta" structures [2,3].

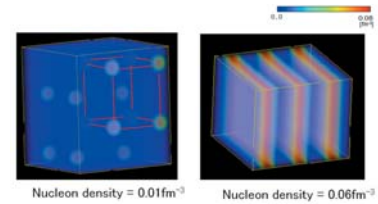

Fig. 1 Examples of "pasta" structures by a fully three-dimensional calculation.

To understand LG mixed phase in more detail, we have performed a fully three-dimensional calculation without assuming geometrical symmetry in the structure. As shown in Fig. 1, we have observed typical "pasta" structures, which was expected in the studies which assume geometrical symmetry. On the other hand we have observed more complex structures with networks of matter or mixture of two kinds of pasta structures. They may emerge as the meta-stable states of matter.

References

[1] K. Shirotori, Ph.D thesis, Tohoku Univ. (2011).
[2] T. Maruyama, N. Yasutake, and T. Tatsumi, Prog. Theor. Phys. Suppl. **186**, 69 (2010).
[3] T. Maruyama, T. Tatsumi, and S. Chiba, Nucl. Phys. A **834**, 561c (2010).

Research Group for Bioactinide

Group Leader: Toshihiko Ohnuki

Our research subject is focused on the formation of actinides and lanthanides nano-particles in the biological reaction environments. The central objectives are to elucidate the biological and chemical processes of the nano-particles formation by analyzing change on chemical states of acitinides by advanced analytical methods. Among the interaction of actinides and lanthnides with microorganisms, nano-particle formation by the transfer of phosphorous ions and electron from the cells to actinides has been studied.

Formation of phosphate nano-particles in the biological reaction environments

Phosphate minerals containing heavy elements of lanthanides and U are known to be hardly soluble in the aqueous solution in the environments. Phosphorous is an essential element of microorganisms. The microorganisms store P in their cells. We have found that yeast, *Saccharomyces cerevisiae* releases P in solution containing U(VI), followed by the formation of uranyl phosphate mineral of H-autunite [1]. However, not only mechanism of the formation of uranyl phosphate mineral, but role of microorganisms for the formation have not been elucidated.

We have conducted the research of phosphate mineralization of one of the lanthanide elements of Ce on the cell surface of yeast [2]. The yeast cells were exposed to Ce containing solution. Cerium concentration in solutions decreases as a function of exposure time. Analyses of the yeast cells by FESEM, TEM, and XAFS show that needle-shaped Ce(III) phosphate nanocrystallites with a monazite structure formed on the yeast cells by exposure to Ce(III) for 42 h, even though the initial solutions did not contain any P species. The Ce(III) phosphate nanocrystals grew from about 50 nm to hundreds of nanometers. P concentration in the solution increased after the yeast cells were inoculated, indicating the release of P from the yeast cells. These results suggest that the sorbed Ce on the cell surfaces reacted with P released from inside the yeast cell, resulting in the formation of Ce(III) phosphate nanocrystallites.

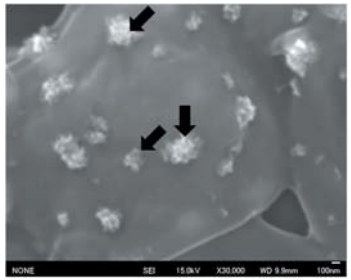

Fig. 1 SEM image the precipitates formed on the yeast cell surface after exposure to 1.79 × 10^{-4} mol·L^{-1} of Ce solution for 7 days at pH 5. Bright spots sized 100-200 nm with black arrow are observed on the cell.

Formation of nano-particles by electron transfer in the biological reaction environments

Electron is transferred when microorganisms respire to obtain energy. Some microorganisms, i.e. iron reducing bacteria, can reduce soluble U(VI) to insoluble U(IV) using organic substrates or hydrogen as electron donor. By the reduction of U(VI) to U(IV), nano-particles of UO_2 have been formed. However, mechanism of the formation of UO_2 nano particles have not been elucidated. In this year, we have examined the electron pathway for the U(VI) reduction mediated by flavin mononucleotide (FMN), which is secreted by *Shewanella* species [3].

The cyclic voltammetry (CV) and photo-electrochemical methods with an optically transparent thin-layer electrode (OTTLE) cell were utilized in investigating in vitro the electron transfer reactions that take place between FMN and U(VI). In the CV measurements of U(VI), a catalytic U(VI) reduction current was observed in the presence of FMN at the redox potential of the FMN. The reduction current increased with an increase in the concentration of the U(VI). The reduced form of the U was confirmed to be U(IV) by the photo-electrochemical analysis using the OTTLE cell. The results demonstrated that FMN acts as the mediator in the electro-reduction of U(VI) to U(IV). In addition, in-vivo bio-reduction experiments on U(VI) with *Shewanella putrefaciens* revealed that the addition of FMN accelerated the reduction rate of the U(VI). These results indicate that the bio-reduction of U(VI) by the *Shewanella* species can be catalyzed by FMN secreted from the cells.

Electron transfer from Mn(II) to manganese oxidizing microorganisms causes the formation of Mn(IV) oxides. Manganese oxides have oxidizing properties for Ce(III). The oxidation of Ce(III) by Mn oxides causes positive Ce adsorption anomaly in the rare earth elements (REE) [4]. We have found that the positive Ce anomaly for the biogenic Mn oxide detected at pH 3.83 decreases with increasing pH. Suppression of the positive Ce anomaly under higher pH is recognized for the biogenic Mn oxide, and further negative Ce anomaly is observed at a pH of more than 6.5 [5]. The trend observed for our data is quite opposite to that observed for the previous studies using abiotically synthesized Mn oxide, where the degree of positive Ce anomaly increases with increasing pH. The detail of the research results is shown in the research highlight.

References

[1] T. Ohnuki *et al.*, Geochim. Cosmochim. Acta **69**, 5307 (2005).
[2] M. Jiang *et al.*, Chem. Geol. **277**, 61 (2010).
[3] Y. Suzuki *et al.*, Phys. Chem. Chem Phys. **12**, 10081 (2010).
[4] A. Ohta *et al.*, Geochim. Cosmochim. Acta **65**, 695 (2001).
[5] K. Tanaka *et al.*, Geochim. Cosmochim. Acta **74**, 5463 (2010).

Research Group for Radiation and Biomolecular Science

Group Leader: Akinari Yokoya

The research objective of Radiation and Biomolecular Science Group is to fully characterize molecular processes by which ionizing radiation alters the chemical structure of biomolecules, particularly the genetic material (DNA), in cells. Two approaches are proposed to address the main objective: 1) Determine the physicochemical processes of DNA alteration induced by radiation in terms of electron/hole transfer within DNA and the hydrated water layer surrounding DNA. 2) Obtain experimental evidence of cellular responses to radiation, including DNA repair processes to various types of DNA alteration in living cells.

Study of unpaired electron species in pyrimidine DNA-bases induced by nitrogen and oxygen *K*-shell photoabsorption

In order to clarify the mechanism of DNA-base modification (base lesion) induced by *K*-shell photoabsorption of nitrogen and oxygen atoms, we have developed an X-band electron paramagnetic resonance (EPR) spectrometer system at a synchrotron soft X-ray beamline BL23SU in SPring-8, and examined the EPR '*in situ*' signal during the soft X-ray irradiation. Spectra of two DNA pyrimidine bases, thymine and cytosine, were measured and their fine structures around nitrogen and oxygen *K*-edges were observed. The *g*-factor of the short-lived unpaired electron arising only during irradiation in thymine was determined to be 2.000, which is distinct from that of a free electron (2.0023). The EPR intensities for cytosine are significantly enhanced by nitrogen (Fig. 1) and oxygen *K*-absorption, indicating that cytosine favors to form unpaired electron species, rather than thymine, presumably due to the excitation of the enhanced electron capturing [1].

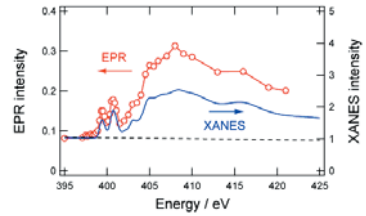

Fig. 1 Dependence of the EPR intensity of cytosine film on soft X-ray energy around nitrogen *K*-edge. The right-hand axis shows the intensity of the X-ray absorption near edge structure (XANES) spectrum. The dotted line represents the baseline deduced from the calculation of the photoabsorption cross section of cytosine assuming that the cross section is determined by summing up each elements cross sections, without nitrogen *K*-shell.

The significance of a base modification with a GAP type strand break within a clustered DNA damage site on the induction of mutations

Base lesion(s) induced by high LET radiation associated with other types of damage, known as a clustered DNA damage site, compromise(s) base excision repair proteins [2]. The effect of clustered DNA damage sites *in vivo* still remains largely unknown. We examined whether two- or three-lesion clustered damage site containing an 8-oxoG(s) and a single strand break (SSB) with hydroxyl groups at the both strand-break termini (called "GAP" type SSB) is highly mutagenic, using plasmid based assay in *Escherichia coli (E.coli)* to musure mutation frequency of these clsutered DNA damage sites [3]. The experimentaly determined mutation frequencies of bi-stranded two-lesion clusters (GAP/8-oxoG), especially in *mutY* deficient *Escherichia coli* strain, are high or are similar to those for bi-stranded clusters with 8-oxoG and other base modifications, such as dihydrothymine, or abasic site (AP site), suggesting that the GAP is processed at similar efficiencies with 8-oxoG or AP site within a cluster. The mutation frequencies of tandem two-lesion clusters comprised of an 8-oxoG and a GAP are, on the other hand, comparable to or less than that of single 8-oxoG. Mutagenic potential of three lesion clusters, which were comprised of a tandem lesion (an 8-oxoG and a GAP) and an opposing single 8-oxoG, was higher than that of a single 8-oxoG but was no more than that of a bi-stranded 8-oxoGs. We suggest that although the nucleotide incorporation opposite 8-oxoG plays an important role, it is less, at least in part, mutagenic when GAP is present on the opposite strand. Our observations indicate that the repair of a GAP is retarded by opposing, but not by tandem, 8-oxoG and that the extent of GAP repair determines the biological consequences.

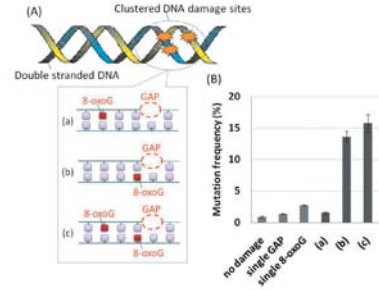

Fig. 2 Mutation frequencies of two- or three- lesion clustered damage sites containing 8-oxoG(s) and a GAP transformed into *mutY* deficient strain of *E.coli*. (A), scheme of three types of clustered damage sites on double stranded DNA. (B), mutation frequencies of these clustered damage sites transformed into *mutY* deficient strain of *E.coli*.

References

[1] T. Oka *et al.*, Appl. Phys. Lett. **98**, 103701 (2011).
[2] A. Yokoya *et al.*, *in Charged Particle and Photon Interactions with Matter*, ed. by Y. Hatano, Y. Katsumura, and A. Mozumder (CRC Press, 2011), Chap. 20, p. 543
[3] N. Shikazono *et al.*, J. Radiat. Res. **50**, 27 (2009).

Research Group for Spin-polarized Positron Beam

Group Leader: Atsuo Kawasuso

Primary target of our research project is the establishment of a highly spin-polarized positron beam for the research on spin-electronic materials. We produce intense positron source (^{68}Ge-^{68}Ga) that yields much highly polarized positrons than the conventional ^{22}Na source through nuclear reactions. We perform the spin-polarized positron annihilation experiments. Employing previously developed reflection high-energy positron diffraction (RHEPD) and Positron microsope, we also promote the studies of surface low-dimensional materials and nuclear materials.

Spin-polarized electrons in Fe, Co, Ni and Gd detected by spin-polarized positron annihilation

The electron momentum distribution of a magnetic substance observed using spin-polarized positrons exhibits so-called field-reversal asymmetry as shown in Fig. 1 due to time-reversal symmetry breaking arising from excess electron spins [1]. The Doppler broadening of annihilation radiation (DBAR) spectra of Fe, Co, Ni, and Gd polycrystals measured using spin-polarized positrons from a ^{68}Ge-^{68}Ga source in magnetic fields exhibited clear asymmetry upon field reversal. The differential DBAR spectra between field-up and field-down conditions were reproduced in calculations considering polarization of positrons and electrons. The magnitudes of the field-reversal asymmetry for the Fe, Co, and Ni samples were approximately proportional to the effective magnetization. The magnetic field dependence of the DBAR spectrum for the Fe sample showed hysteresis that is similar to a magnetization curve. These results demonstrate that spin-polarized positron annihilation spectroscopy will be useful in studying magnetic properties of spin-electronic materials.

Atomic configuration of two-dimensional electron compound revealed by RHEPD

The adsorption of the noble and alkali metal atoms on the Si(111)-$\sqrt{3}\times\sqrt{3}$-Ag surface leads to the formation of $\sqrt{21}\times\sqrt{21}$ superstructures, accompanied by the drastic increase in the surface electrical conductivity. Recently, we found that the $\sqrt{21}\times\sqrt{21}$ superstructures are fabricated with different stoichiometry of the adsorbed binary metal atoms on the Si(111) surface. The atomic and electronic structures of the Au and Ag superstructure have been investigated using reflection high-energy positron diffraction (RHEPD), angle-resolved photoemission spectroscopy (ARPES), scanning tunnelling microscopy (STM), and semi-empirical theoretical approach [2]. As a result, we found that the Si(111)-$\sqrt{21}\times\sqrt{21}$ superstructure has a characteristic of electron compounds. We also found that the interaction energy among the adsorbates plays an important role in the formation of $\sqrt{21}\times\sqrt{21}$ superstructures.

This work was done in collaboration with Matsuda group of ISSP, University of Tokyo.

Stress-induced corrosion cracking observed by positron microscope

Stress corrosion cracking (SCC) is still an important issue in the low-carbon austenitic stainless steels developed as corrosion resistive materials for nuclear power plants. However, its mechanism has not yet fully been clarified. Recently, a hypothesis of the SCC crack propagation mediated by vacancy defects in a stress field near the crack tip is proposed. To investigate the vacancy formation during the SCC crack propagation, vacancy defects near the crack tip in stainless steel under tensile stress has been observed through *in-situ* positron microbeam measurements [3]. From the DBAR measurements of a stress-corrosion-cracked stainless steel, a clear increase of density of vacancy defects was observed over 200-400 μm areas from the SCC crack. From the comparison of the DBAR spectra obtained for the SCC sample and plastically deformed sample, the vacancy defects around the SCC crack were attributed to plastic deformation due to the stress concentration near the crack tip [4]. On the other hand, it is reported that vacancy defects in austenitic stainless steels migrate easily at a high temperature and move along the tensile stress. Crack progress by the SCC may occur preferentially in the crack tip where vacancy defects are accumulated

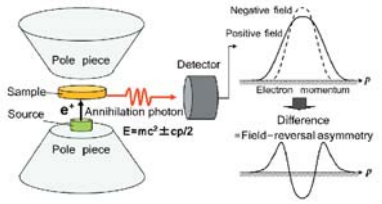

Fig. 1 Principle of spin-polarized positron annihilation spectroscopy (SP-PAS). Sample and source are placed in magnetic field. Longitudinally polarized positrons from the source are implanted into the magnetized sample and annihilation photons are detected by a Ge detector. Thus obtained DBAR spectrum reflects the electron momentum distribution. DBAR spectra for the field-up and field-down conditions are not identical due to the different spin statistics between positrons and electrons upon field reversal. This is called the field-reversal asymmetry. Field dependence of DBAR spectrum provides information on effective magnetization, electron spin-polarization and magnetization property of a magnetic substance. Considering the fact that positrons are trapped by vacancy defects, magnetisms induced by vacancy defects will be studied by SP-PAS method. By developing low-energy polarized positron beam, magnetic thin films and spin phenomena near surface will also be studied.

References

[1] A. Kawasuso *et al*., Phys. Rev. B **83**, 100406(R) (2011).
[2] I. Matsuda *et al*., Phys. Rev. B **82**, 165330 (2010).
[3] M. Maekawa, A. Yabuuchi, and A. Kawasuso, J. Phys. : Conf.Ser. **225**, 012033 (2010).
[4] A. Yabuuchi, M. Maekawa, and A. Kawasuso, J. Phys. : Conf.Ser. **262**, 012067 (2011).

Publication List

Research Group for Condensed Matter Theory

Papers

1) Extremely long quasiparticle spin lifetimes in superconducting aluminium using MgO tunnel spin injectors, H. Yang, S. H. Yang, S. Takahashi, S. Maekawa, S.S.P. Parkin, *Nature Materials* **9**, 586-593 (2010).
2) Spin Seebeck insulator, K. Uchida, J. Xiao, H. Adachi, J. Ohe, S. Takahashi, J. Ieda, T. Ota, Y. Kajiwara, H. Umezawa, H. Kawai, G. E.W. Bauer, S. Maekawa and E. Saitoh, *Nature Materials* **9**, 894-897 (2010).
3) Quantum Renormalization of the Spin Hall Effect, B. Gu, J. Y. Gan, N. Bulut, T. Ziman, G. Y. Guo, N. Nagaosa, and S. Maekawa, *Phys. Rev. Lett* **105**, 086401-1-086401-4 (2010).
4) Surface-assisted spin Hall effect in Au films with Pt impurities, B. Gu, I. Sugai, T. Ziman, G. Y. Guo, N. Nagaosa, T. Seki, K. Takanashi, and S. Maekawa, *Phys. Rev. Lett.* **105**, 216401-1-216401-4 (2010).
5) Enhanced pairing correlations near oxygen dopants in cuprate superconductors, G. Khaliullin, M. Mori, T. Tohyama, and S. Maekawa, *Phys. Rev. Lett.* **105**, 257005-1-257005-4 (2010).
6) Observation of longitudinal spin-Seebeck effect in magnetic insulators, K. Uchida, H. Adachi, T. Ota, H. Nakayama, S. Maekawa and E. Saitoh, *Appl. Phys. Lett.* **97**, 172505-1-172505-3 (2010).
7) Gigantic enhancement of spin Seebeck effect by phonon drag, H. Adachi, K. Uchida, E. Saitoh, J. Ohe, S. Takahashi, and S. Maekawa, *Appl. Phys. Lett.* **97**, 252506-1-252506-3 (2010).
8) Dynamics of attractively interacting fermi atoms in one-dimensional optical lattices: Non-equilibrium simulations of fermion superfluidity, M. Okumura, H. Onishi, S. Yamada, and M. Machida, *Physica C* **470**, S949-S951 (2010).
9) Anomalous non-equilibrium electron transport in one-dimensional quantum nano wire at half-filling: time dependent density renormalization group study, M. Okumura, H. Onishi, S. Yamada, and M. Machida, *J. Phys.: Conf. Ser.* **248**, 012031-1-012031-7 (2010).
10) Effects of Mechanical Rotation on Spin Currents, M. Matsuo, J. Ieda, E. Saitoh, and S. Maekawa, *Phys. Rev. Lett.* **106**, 076601-1-076601-4 (2011).
11) Thermoelectric response in the incoherent transport region near Mott transition: the case study of $La_{1-x}Sr_xVO_3$, M. Uchida, K. Oishi, M. Matsuo, W. Koshibae, Y. Onose, M. Mori, J. Fujioka, S. Miyasaka, S. Maekawa, and Y. Tokura, *Phys. Rev. B* **83**, 165127-1-165127-5 (2011).
12) Numerical study on the spin Seebeck effect, J. Ohe, H. Adachi, S. Takahashi, and S. Maekawa, *Phys. Rev. B* **83**, 115118-1-115118-5 (2011).
13) Linear-response theory of spin Seebeck effect in ferromagnetic insulators, H. Adachi, J. Ohe, S. Takahashi, and S. Maekawa, *Phys. Rev. B* **83**, 094410-1-094410-6 (2011).
14) Giant spin Hall effect of Au films with Pt impurities: Surface-assisted skew scattering, B. Gu, T. Ziman, G. Y. Guo, N. Nagaosa, and S. Maekawa, *J. Appl. Phys.* **109**, 07C502-1-07C502-3 (2011).
15) Equation-of-motion approach of spin-motive force, Y. Yamane, J. Ieda, J. Ohe, S. E. Barnes, and S. Maekawa, *J. Appl. Phys.* **109**, 07C735-1-07C735-3 (2011).
16) Spin transfer torque in MTJs with synthetic ferrimagnetic layers by the Keldysh approach, M. Ichimura, T. Hamada, H. Imamura, S. Takahashi, and S. Maekawa, *J. Appl. Phys.* **109**, 07C906-1-07C906-3 (2011).
17) Microwave-induced supercurrent in a ferromagnetic Josephson junction, S. Hikino, M. Mori, S. Takahashi, and S. Maekawa, *Supercond. Sci. Technol.* **24**, 024008-1-024008-5 (2011).

Books & Reviews

1) From GMR to TMR, S. Maekawa, and J. Ieda, *BUTSURI* **65**, 324-330 (2010) (*in Japanese*).
2) New Interplay of Spin and Heat, H. Adachi, and S. Maekawa, *Magnetics Jpn* **5**, 256-263 (2010) (*in Japanese*).
3) New numerical approach for studying diluted magnetic semiconductors, J. Ohe, B. Gu, and S. Maekawa, *KOTAIBUTSURI* **45**, 269-278 (2010) (in Japanese).

Invited Talks

1) Possible mechanisms of enhanced pairing gap near apical and dopant oxygens in cuprate, M. Mori, *The 9th Asia Pacific Workshop on Materials Physics*, Hanoi, Vietnam (2010).
2) Spin-wave spin current in non-equilibrium systems, J. Ohe, *KIST Spintronics workshop*, Seoul, Korea (2010).
3) Spin motive force induced by the magnetic vortex core motion, J. Ohe, *International Conference of AUMS (ICAUMS2010)*, Jeju, Korea (2010).
4) Enhanced pairing correlation near oxygens in cuprate, M. Mori, *Super-PIRE/REIMEI workshop*, Knoxville, USA (2010).
5) Quantum transport in nano-structure of superconductor and ferromagnet, M. Mori, *ARW Workshop Hvar 2010*, Hvar, Croatia (2010).
6) Spin Current, Charge Current and their Interaction in Magnetic Nanostructures, S. Maekawa, *The 9th Asia Pacific Workshop on Materials Physics (APW2010)*, Hanoi, Vietnam (2010).
7) Spin-Wave Spin Current as a Transmission Tool of Electric Signal and Thermal Energy, S. Maekawa, *International Conference of AUMS (ICAUMS2010)*, Jeju, Korea (2010).
8) Spin-Wave Spin Current as a Transmission Tool of Electric Signal and Thermal Energy, S. Maekawa, *CRP Workshop on Oxide Electronics*, Singapore (2010).
9) Seebeck Effect, Spin Seebeck Effect and Spin-Electronics, S. Maekawa, *APW Workshop Hvar 2010*, Hvar, Croatia (2010).
10) Seebeck Effect, Spin Seebeck Effect and Spin-Electronics, S. Maekawa, *RIKEN Opening Symposium of QS2C Theory Forum*, Wako, Japan (2010).
11) Spin Current, Charge Current and their Interaction in Magnetic Nanostructures, S. Maekawa, *The 34th conference of The Magnetic Society of Japan, Tsukuba*, Japan (2010).
12) Spin-Wave Spin Current as a Transmission Tool of Electric Signal and Thermal Energy, S. Maekawa, *Spin Age 2010*, California, USA (2010).
13) Spin injection into a superconductor, S. Maekawa, *Shanghai Workshop on Spintronics and Low Dimensional Magnetism*, Shanghai, China (2010)
14) Spin Current, Charge Current and their Interaction in Magnetic Nanostructures, S. Maekawa, *KITPC 2010*, Beijing, China (2010).
15) Seebeck Effect, Spin Seebeck Effect and Spin-Electronics, S. Maekawa, *Workshop on High Performance Ceramic*, Hangzhou, China (2010).
16) Ferromagnetic Josephson Resonance, S. Maekawa, *SNS 2010*, Shanghai, China (2010).
17) Spin injection into a superconductor in a magnetic double tunnel junction, S. Maekawa, *ESF-NES Workshop 2010*, Salzburg, Austria (2010).
18) Materials Design of Magnetic Semiconductors -Quantum Monte Carlo Study-, S. Maekawa, *NASCES 2011*, Tokai, Japan (2011).

Research Group for Molecular Spintronics

Papers

1) Thermal Effect on Structure Organizations in Cobalt-Fullerene Nanocomposition, V. Lavrentiev, J. Vacik, H. Naramoto and S. Sakai, *J. Nanosci. & Nanotech.* **10**, 2624-2629 (2010).
2) RBS study of diffusion under strong centrifugal force in bimetallic Au/Cu thin films, T. Hao, M. Ono, S. Okayasu, S. Sakai, K. Narumi, Y. Hiraiwa, H. Naramoto and Y. Maeda, *Nucl. Instr. and Meth. in Phys. Res. B* **268**, 1867-1870 (2010).
3) Composition dependence of magnetic and magnetotransport properties in C_{60}-Co granular thin films, I. Sugai, S. Sakai, Y. Matsumoto, H. Naramoto, S. Mitani, K. Takanashi, and Y. Maeda, *J. Appl. Phys.* **108**, 063920-1-6 (2010).
4) Effect of ion irradiation on structure and thermal evolution of the Ni-C_{60} hybrid systems, J. Vacik, V. Lavrentiev, V. Vorlicek, L. Bacakova, and K. Narumi, *Nucl. Instr. and Meth. in Phys. Res. B* **268**, 1976-1979 (2010).
5) Observation of intermolecular N-I interaction during the growth of a 4-cyano-4'-iodobiphenyl molecular crystal on GeS(001), R. Sumii, M. Sakamaki, Y. Matsumoto, K. Amemiya, K. Kanai, and K. Seki, *Surf. Sci.* **604**, 1100-1104 (2010).
6) Interface Properties of Metal/Graphene Heterostructures Studied by Micro-Raman Spectroscopy, S. Entani, S. Sakai, Y. Matsumoto, H. Naramoto, T. Hao, and Y. Maeda, *J. Phys. Chem. C* **114**, 20042-20048 (2010).
7) Comparison of secondary ion emission yields for poly-tyrosine between cluster and heavy ion impacts, K. Hirata, Y. Saitoh, A. Chiba, K. Yamada, Y. Takahashi, and K. Narumi, *Nucl. Instr. and Meth. in Phys. Res. B* **268**, 2930-2932 (2010).
8) Atomic Structure and Energetic Stability of Complex Chiral Silicon Nanowires, P. V. Avramov, S. Minami, S. Irle, L. A. Chernozatonskii, and K. Morokuma, *J. Phys. Chem. C* **114**, 14692-14696 (2010).
9) Theoretical Study of Atomic Structure and Elastic Properties of Branched Silicon Nanowires, P. B. Sorokin, A. G. Kvashnin, D. G. Kvashnin, J. A. Filicheva, P. V. Avramov, and A. S. Fedorov, *ACS Nano* **4**, 2784-2790 (2010).
10) Theoretical Study of Elastic Properties of SiC Nanowires of Different Shapes, P. B. Sorokin, D. G. Kvashnin, A. G. Kvashnin, P. V. Avramov, and L. A. Chernozatonskii, *J. Nanosci. & Nanotech.* **10**, 4992-4997 (2010).
11) Beta-phase silicon nanowires: structure and electronic properties, P. B. Sorokin, P. V. Avratonov, V. A. Demin, and L. A. Chernozatonskii, *JETP Letters* **92**, 352-355 (2010).
12) Determination of silicon vacancy in ion-beam synthesized β-$FeSi_2$, Y. Maeda, T. Ichikawa, T. Jonishi, and K. Narumi, *Physics Procedia* **11**, 83-86 (2011).
13) Size-derived effects in electronic and elastic properties of diamanes, L. A. Chernozatonskii, P. B. Sorokin, A. A. Kuzubov, B. P. Sorokin, A. G. Kvashnin, D. G. Kvashnin, P. V. Avramov, and B. I. Yakobson, *J. Phys. Chem. C* **115**, 132-136 (2011).

Books & Reviews

1) The elastic properties of branched silicon nanowires: the theoretical study, P. B. Sorokin, A. G. Kvashnin, D. G. Kvashnin, P. V. Avramov, and L. A. Chernozatonskii, *Handbook of Chemistry, Biochemistry and Biology: New Frontiers*, 331-336, Nova Publishers (2010).
2) The study of the atomic structure and elastic properties of the silicon carbide nanowires, P. B. Sorokin, A. G. Kvashnin, D. G. Kvashnin, P. V. Avramov, and L. A. Chernozatonskii, *Handbook of Chemistry, Biochemistry and Biology: New Frontiers*, 325-330, Nova Publishers (2010).

Invited Talks

1) Spin polarization of organic molecules on magnetic surfaces probed by a metastable helium beam, Y. Yamauchi, *18th International Workshop on Inelastic Ion-Surface Collisions*, Gatlinburg, USA (2010).
2) Spintronic application and structure design of molecules and nanocarbons by quantum-beams, S. Sakai, *5th Takasaki Advanced Radiation Research Symposium*, Takasaki, Japan (2010).

3) Spin-dependent transport and electronic/magnetic structures in fullerene-magnetic metal systems, S. Sakai, *The 32th Special Meeting on Spin-electronics of the Magnetic Society of Japan*, Kyoto, Japan (2010).
4) Ion-Beam Analysis of Bombardment Effect of 10-to-100-keV C60 Ions on a Si Surface, K. Narumi, *11th Special Meeting on Surface and Interface Analysis by Ion-Beam*, Nagoya, Japan (2010).
5) Spin states of molecules and nanocarbons analyzed by X-ray magnetic dichroism spectroscopy, Y. Matsumoto, *Photon Factory Meeting*, Tsukuba, Japan (2011).
6) Analysis of electronic and spin states in nanocarbon- and molecule-magnetic metal systems for spintronic application, Y. Matsumoto, *17th Meeting on Silicide Semiconductors and Related Materials*, Tokyo, Japan (2011).
7) Growth of graphene on magnetic metal surface and its spin polarization measurements, S. Entani, *17th Meeting on Silicide Semiconductors and Related Materials*, Tokyo, Japan (2011).

Research Group for Mechanical Control of Materials and Spin Systems

Papers
1) Modulation of Gyromagnetic Ratio in $Ni_{81}Fe_{19}$ Thin Film Due to Spin Pumping, K. Sasage, K. Harii, K. Ando, K. Uchida, and E. Saitoh, *J. Magn. Mater.* **322**, 1425-1427 (2010).
2) Angular dependence of inverse spin-Hall effect induced by spin pumping: experimental verification of phenomenological model of spin pumping, K. Ando, T. Yoshino, N. Okamoto, Y. Kajiwara, K. Sasage, K. Uchida, and E. Saitoh, *J. Magn. Mater.* **322**, 1422-1424 (2010).
3) Electric detection of the spin-Seebeck effect in ferromagnetic metals, K. Uchida, T. Ota, K. Harii, K. Ando, H. Nakayama, and E. Saitoh, *J. Appl. Phys.* **107**, 09A951-1-09A951-5 (2010).
4) Direct conversion of light-polarization information into electric voltage using photoinduced inverse spin-Hall effect in Pt/GaAs hybrid structure: Spin photodetector, K. Ando, M. Morikawa, T. Trypiniotis, Y. Fujikawa, C. H. W. Barnes, and E. Saitoh, *J. Appl. Phys.* **107**, 113902-1-113902-5 (2010).
5) Inverse spin-Hall effect induced by spin pumping in various metals, K. Ando, Y. Kajiwara, K. Sasage, K. Uchida, and E. Saitoh, *IEEE transactions on magnetics*. **46**, 1331 – 1333 (2010).
6) Inverse spin-Hall effect induced by spin pumping in different thickness Pt films, H. Nakayama, K. Ando, K. Harii, Y. Kajiwara, T. Yoshino. K. Uchida, and E. Saitoh, *IEEE Trans. Magn.* **46**, 2202-2204 (2010).
7) Spin Seebeck insulator, K. Uchida, J. Xiao, H. Adachi, J. Ohe, S. Takahashi, J. Ieda, T. Ota, Y. Kajiwara, H. Umezawa, H. Kawai, G. E. W. Bauer, S. Maekawa, and E. Saitoh, *Nat. Mater.* **9**, 894-897 (2010).
8) Observation of longitudinal spin-Seebeck effect in magnetic insulators, K. Uchida, H. Adachi, T. Ota, H. Nakayama, S. Maekawa, and E. Saitoh, *Appl. Phys. Lett.* **96**, 172505-1-172505-3 (2010).
9) Inverse spin-Hall effect in palladium at room temperature, K. Ando and E. Saitoh, *J. Appl. Phys.* **108**, 113925-1-113925-4 (2010).
10) Enhancement of the spin pumping efficiency by spin wave mode selection, C. W. Sandweg, Y. Kajiwara, K. Ando, E. Saitoh, and B. Hillebrands, *Appl. Phys. Lett.* **97**, 252504-1-252504-3 (2010).
11) Gigantic enhancement of spin Seebeck effect by phonon drag, H. Adachi, K. Uchida, E. Saitoh, J. Ohe, S. Takahashi, and S. Maekawa, *Appl. Phys. Lett.* **97**, 252506-1-252506-3 (2010).
12) Longitudinal spin-Seebeck effect in sintered polycrystalline (Mn,Zn)Fe2O4, K. Uchida, T. Nonaka, T. Ota, and E. Saitoh, *Appl. Phys. Lett.* **97**, 262504-1-262504-3 (2010).
13) Spin current study of spin glass AgMn using spin pumping effect, R. Iguchi, K. Ando, E. Saitoh, and T. Sato, *J. Phys.: Conf. Ser.* **266**, 012089-1-012089-4 (2011).
14) Inverse spin-Hall effect induced by spin pumping in different size $Ni_{81}Fe_{19}$/Pt films, H. Nakayama, K. Ando, K. Harii, Y. Fujikawa, Y. Kajiwara, T. Yoshino, and E. Saitoh, *J. Phys.: Conf. Ser.* **266**, 012100-1-012100-4 (2011).
15) Spin pumping and magnetization-precession trajectory in thin film systems, T. Nonaka, K Ando, T. Yoshino, and E Saitoh, *J. Phys.: Conf. Ser.* **266**, 012101-1-012101-4 (2011).
16) Quantifying spin mixing conductance in F/Pt (F =Ni, Fe, and $Ni_{81}Fe_{19}$) bilayer film, T Yoshino, K Ando, K Harii, H Nakayama, Y Kajiwara and E Saitoh, *J. Phys.: Conf. Ser.* **266**, 012115-1-012115-4 (2010).
17) Effects of mechanical rotation on spin currents (selected as Editor's Suggestion), M. Matsuo, J. Ieda, E. Saitoh, and S. Maekawa, *Phys. Rev. Lett.* **106**, 076601-1-076601-4 (2011).
18) Spin Pumping Efficiency from Half Metallic Co_2MnSi, H. Chudo, K. Ando, K. Saito, S. Okayasu, R. Haruki, Y. Sakuraba, H. Yasuoka, K. Takanashi, and E. Saitoh, *J. Appl. Phys.* **109**, 073915-1-073915-4 (2011)
19) Scanning SQUID Microscope Study of Vortex Polygons and Shells in Weak Pinning Disks of an Amorphaous Thin Film, N. Kokubo, S. Okayasu, A. Kanda, and B. Shinozaki, *Phys. Rev. B* **82**, 014501-1-014501-8 (2010).
20) Deformation twinning of Bi–Sb solid alloy formed under a strong gravitational field, *Philos. Mag. Lett.*, **90**, 513-518 (2010).
21) Investigation on new scintillators for subnanosecond time-resolved x-ray measurements, R. Haruki, K. Shibuya, F. Nishikido, M. Koshimizu, Y. Yoda, and S. Kishimoto, *J. Phys. Conf. Ser.* **217**, 012007-1-012007-4 (2010).
22) Effect of strong gravity on $Y_1Ba_2Cu_3O_{7-\delta}$ superconductor, R. Bagum, A. Yoshiasa, S. Okayasu, Y. Iguchi, M. Ono, M. Okube and T. Mashimo, *J. Appl. Phys.* **108**, 053517-1-053517-7 (2010).
23) Anisotropic Spin Fluctuations in Heavy-Fermion Superconductor $NpPd_5Al_2$, H. Chudo, H. Sakai, Y. Tokunaga, S. Kambe, D. Aoki, Y. Homma, Y. Haga, T. D. Matsuda, Y. Ōnuki, and H. Yasuoka, *J. Phys. Soc. Jpn.* **79**, 053704-1-053704-4 (2010).
24) Evidence for Appearance of an Internal Field in the Ordered State of $CeRu_2Al_{10}$ by μ^+SR, S. Kambe, H. Chudo, Y. Tokunaga, T. Koyama, H. Sakai, T. U. Ito, K. Ninomiya, W. Higemoto, T. Takesaka, T. Nishioka, and Y. Miyake, *J. Phys. Soc. Jpn.* **79**, 053708-1-053708-3 (2010).
25) NMR Evidence for the 8.5 K Phase Transition in Americium Dioxide, Y. Tokunaga, T. Nishi, S. Kambe, M. Nakada, A. Itoh, Y. Homma, H. Sakai, and H. Chudo, *J. Phys. Soc. Jpn.* **79**, 053705-1-053705-4 (2010).
26) La substitution effect and hyperfine-enhanced ^{141}Pr nuclear spin dynamics in $PrPb_3$: ^{139}La NMR study in $Pr_{0.97}La_{0.03}Pb_3$, Y. Tokunaga, H. Sakai, H. Chudo, S. Kambe, H. Yasuoka, H. S. Suzuki, R. E. Walstedt, Y. Homma, D. Aoki, and Y. Shiokawa, *Phys. Rev. B* **82**, 104401-1-104401-6 (2010).
27) Energy scale of the electron-boson spectral function and superconductivity in $NpPd_5Al_2$, G. A. Ummarino, R. Caciuffo, H. Chudo and S. Kambe, *Phys. Rev. B* **82**, 104510-1-104510-7 (2010).
28) One-component description for magnetic excitations in heavy fermion $CeIrIn_5$, S. Kambe, Y. Tokunaga, H. Sakai, H. Chudo, Y. Haga, T.D. Matsuda and R.E. Walstedt, *Phys. Rev. B* **81**, 140405(R)-1-140405(R)-4 (2010).

Books & Reviews
1) Observation of Spin Seebeck Effects in ferromagnetic metals, K. Uchida and E. Saitoh, *MAGUNE 5*, 283-289 (2010) (*in Japanese*).
2) Spintronics Phenomena associated with thermal current, K. Uchida and E. Saitoh, MATERIA 49, 357-363 (2010) (*in Japanese*).
3) Spin Current Transmission using magnetic insulator, Y. Kajiwara, K. Ando and E. Saitoh, MATERIA 49, 575-579 (2010) (*in Japanese*).
4) Progress on Spin Current Science, E. Saitoh, PARITY 26, 32-33 (2011) (in *Japanese*).

Invited Talks
1) Spin Hall and spin Seebeck effects, E.Saitoh, Third International Conference on Nanospintronics Design and Realization, Osaka , Japan (2010).
2) Spin current generation and detection, E.Saitoh, Progress in Spintronics and Graphene Research, Kavli Institute for Theoretical Physics China at the Chinese Academy of Sciences, Beijing, China (2010).
3) Spin current detection and generation using spin-Hall effect, E.Saitoh, Ninth International Workshop on Surface, Interface and Thin Film Physics, Shanghai, Chaina (2010).
4) Spin Seebeck effect, E.Saitoh, 3rd International Conference on Spintronics Materials and Technology, Illinois, USA (2010).
5) Spintronics and spin current, E. Saitoh, 3rd International Conference on Spintronics Materials and Technology, 29th Electronic Materials Symposium, Shizuoka, Japan (2010).
6) Spin Seebeck Effect, E. Saitoh, MSJ 173th Workshop, Tokyo, Japan (2010).
7) Spin Seebeck effect, E.Saitoh," Gordon Research Conferences, Magnetic Nanostructures, Lewiston, USA (2010).
8) Spin and Heat, E. Saitoh, JPS Science Seminar 2010 "Spintronics", Tokyo, Japan (2010).
9) Spin Current Physics, E.Saitoh, 4th IMR-Korea University Seminar, Seoul, Korea (2010).
10) Spin Hall and spin torque effects in metal and insulator films, E.Saitoh, The 34th Annual Conference on MAGNETICS in Japan, Tsukuba, Japan (2010).
11) Development of dielectric spintronic materials and spin optical function, E. Saitoh, The 71st JSAP Fall Meeting, Nagasaki, Japan (2010).
12) Spintronics in Mott insulators, E. Saitoh, The 71st JSAP Fall Meeting, Nagasaki, Japan (2010).
13) Spin current coupled with charge and heat currents, E. Saitoh, The IEEE 7th International Symposium on Metallic Multilayers MML2010, Berkeley (2010).
14) Spin current generation from insulators and metals, E. Saitoh, Magnetism and Magnetic Materials Conference 2010 , Atlanta, USA (2010).
15) Spin current generation and measurements, E. Saitoh, Surface Science Society of Japan, Hamamatsu, Japan (2010).
16) Spin current physics, E. Saitoh, Spintronics Introductory Seminar JSAP Spintronics workshop, Tokyo, Japan (2010).
17) Spin Seebeck effect in metallic materials, E. Saitoh, SORST Symposium, Tokyo, Japan (2011).
18) Spin current generation from metals and insulators, E.Saitoh, International Symposium "Nanoscience and Quantum Physics 2011", Tokyo, Japan (2011).
19) Spintronics and spin current, E. Saitoh, The 20th young forum for Advanced material science, Funabashi, Japan (2011).
20) Spin current generation from insulators and metals, E.Saitoh, The 3rd Scienceweb GCOE International Symposium, Sendai, Japan (2011).
21) Spintronics in Mott Insulators, E. Saitoh, PF Workshop, Tsukuba, Japan (2011).

Research Group for Reactions Involving Heavy Nuclei

Papers
1) A new Type of Asymmetric Fission in Proton-Rich Nuclei, A. N. Andreyev, J. Elseviers, M. Huyse, P. Van Duppen, S. Antalic, A. Barzakh, N. Bree, T. E. Cocolios, V. F. Comas, J. Diriken, D. Fedorov, V. Fedosseev, S. Franchoo, J. A. Heredia, O. Ivanov, U. Koester, B. A. Marsh, K. Nishio, R. D. Page, N. Patronis, M. Seliverstov, I. Tsekhanovich, P. Van den Bergh, J. Van De Walle, M. Venhart, S. Vermote, M. Veselsky, C. Wagemans, T. Ichikawa, A. Iwamoto, P. Moeller, and A. J. Sierk, *Phys. Rev. Lett.* **105**, 252502-1-252502-5 (2010).
2) In-beam γ-ray spectroscopy of ^{248,250,252}Cf by neutron-transfer reactions using a Cf target, R. Takahashi, T. Ishii, M. Asai, D. Nagae, H. Makii, K. Tsukada, A. Toyoshima, Y. Ishii, M. Matuda, A. Makishima, T. Shizuma, T. Kohno, and M. Ogawa, *Phys. Rev. C* **81**, 057303-1-057303-4 (2010).
3) Experimental Study of the ^{238}U(^{36}S,3-5n)$^{269-271}$Hs reaction leading to the observation of ^{270}Hs, R. Graeger, D. Ackermann, M. Chelnokov, V. Chepigin, Ch. E. Duellmann, J. Dvorak, J. Even, A. Gorshkov, F. P. Hessberger, D. Hild, A. Huebner, E. Jaeger, J. Khuyagbaatar, B. Kindler, J. V. Kratz, J. Krier, A. Kuznetsov, B. Lommel, K. Nishio, H. Nitsche, J. P. Omtvedt, O. Petrushkin, D. Rudolph, J. Runke, F. Samadani, M. Schaedel, B. Schausten, A. Tueler, A. Yakushev, and Q. Zhi, *Phys. Rev. C* **81**, 061601(R)-1-061601(R)-5 (2010).
4) Verification of the surrogate ratio method, S. Chiba and O. Iwamoto, *Phys. Rev. C* **81**, 044604-1-044604-6 (2010).
5) New estimate for the time-dependent thermal nucleosynthesis of ^{180}Ta^m, T. Hayakawa, T. Kajino, S. Chiba, and G. J. Mathews, *Phys. Rev. C* **81**, 052801(R)-1-052801(R)-4 (2010).
6) Fusion-fission and quasi-fission process in reactions using actinide target nuclei, Y. Aritomo, *Int. J. Mod. Phys. E* **19**, 813-824 (2010).
7) Nuclear orientation in the reaction ^{34}S + ^{238}U and synthesis of the new isotope ^{268}Hs, K. Nishio, S. Hofmann, F. P. Heßberger, D. Ackermann, S. Antalic, Y. Aritomo, V. F. Comas, Ch. E. Düllmann, A. Gorshkov, R. Graeger, K. Hagino, S. Heinz, J. A. Heredia, K. Hirose, H. Ikezoe, J. Khuyagbaatar, B. Kindler, I. Kojouharov, B. Lommel, R. Mann, S. Mitsuoka, Y. Nagame, I. Nishinaka, T. Ohtsuki, A. G. Popeko, S. Saro, M. Schädel, A. Türler, Y. Watanabe, A. Yakushev, and A. V. Yeremin, *Phys. Rev. C* **82**, 024611-1-024611-9 (2010).
8) Evidence for quasifission in the sub-barrier reaction of ^{30}Si + ^{238}U, K. Nishio, H. Ikezoe, I. Nishinaka, S. Mitsuoka, K. Hirose, T. Ohtsuki, Y. Watanabe, Y. Aritomo, and S. Hofmann, *Phys. Rev. C* **82**, 044604-1-044604-5 (2010).
9) Neutron drip line and the equation of state of nuclear matter, K. Oyamatsu, K. Iida, and H. Koura, *Phys. Rev. C* **82**, 027301-1-027301-4 (2010).
10) Cross-shell excitations near the "island of inversion": Structure of ^{30}Mg, A. N. Deacon, J. F. Smith, S. J. Freeman, R. V. F. Janssens, M. P. Carpenter, B. Hadinia, C. R. Hoffman, B. P. Kay, T. Lauritsen, C. J. Lister, D. O'Donnell, J. Ollier, T. Otsuka, D. Seweryniak, K.-M. Spohr, D. Steppenbeck, S. L. Tabor, V. Tripathi, Y. Utsuno, P. T. Wady, and S. Zhu, *Phys. Rev. C* **82**, 034305-1-034305-7 (2010).
11) Neutrino reactions on ^{138}La and ^{180}Ta via charged and neutral currents by the quasiparticle random-phase approximation, M.-K. Cheoun, E. Ha, T. Hayakawa, T. Kajino, and S. Chiba, *Phys. Rev. C* **82**, 035504-1-035504-7 (2010).
12) Reanalysis of the (J=5) state at 592 keV in ^{180}Ta and its role in the ν-process nucleosynthesis of ^{180}Ta in supernovae, T. Hayakawa, P. Mohr, T. Kajino, S. Chiba, and G. J. Mathews, *Phys. Rev. C* **82**, 058801-1-058801-4 (2010).
13) Novel extrapolation method in the Monte Carlo shell model, N. Shimizu, Y. Utsuno, T. Mizusaki, T. Otsuka, T. Abe, and M. Honma, *Phys. Rev. C* **82**, 061305(R)-1-061305(R)-5 (2010).
14) Decay studies of K isomers in ^{254}No, F. P. Hessberger, S. Antalic, B. Sulignano, D. Ackermann, S. Heinz, S. Hofmann, B. Kindler, J. Khuyagbaatar, I. Kojouharov, P. Kuusiniemi, M. Leino, B. Lommel, R. Mann, K. Nishio, A.G. Popeko, S. Saro, B. Streicher, J. Uusitalo, M. Venhart, and A.V. Yeremin, *Eur. Phys. J. A* **43**, 55-56 (2010).
15) Multi-layered parallel plate ionization chamber for cross-section measurement of minor actinides. K. Hirose, T. Ohtsuki, Y. Shibasaki, N. Iwase, J. Hori, K. Takamiya, H. Yashima, K. Nishio, and Y. Kiyanagi, *Nucl. Instrum. Methods Phys. Res. A* **621**, 379-382 (2010).
16) Extraction chromatographic behavior of Rf, Zr, and Hf in HCl solution with styrene-divinylbenzene copolymer resin modified by TOPO (trictylphosphine oxide), A.Toyoshina, Y. Kasamatsu, K. Tsukada, M. Asai, Y. Ishii, H. Toume, I. Nishinaka, T. K. Sato, Y. Nagame, M. Schädel, H. Haba, S. Goto, H. Kudo, K. Akiyama, Y. Oura, K. Ooe, A. Shinohara, K. Sueki, and J. V. Kratz, *J. Nucl. Radiochem. Sci.* **11**, 7-11 (2010).
17) The new isotope ^{236}Cm and new data on ^{232}Cm and ^{237,238,240}Cf, J. Khuyagbaatar, F.P. Hessberger, S. Hofmann, D. Ackermann, V.S. Comas, S. Heinz, J.A. Heredia, B. Kindler, I. Kojouharov, B. Lommel, R. Mann, K. Nishio, and A. Yakushev, *Eur. Phys. J. A* **46**, 59-67 (2010).
18) Proton resonance elastic scattering in inverse kinematics on the medium heavy nucleus ^{68}Zn, N. Imai, Y. Hirayama, H. Ishiyama, S.C. Jeong, H. Miyatake, Y. X. Watanabe, H. Makii, S. Mitsuoka, D. Nagae, I. Nishinaka, K. Nishio, and K. Yamaguchi, *Eur. Phys. J A* **46**, 157-160 (2010).
19) Multiparticle-multihole states around ^{16}O and correlation-energy effect on the shell gap, Y. Utsuno and S. Chiba, *Phys. Rev. C* **83**, 021301(R)-1-021301(R)-5 (2011).
20) Matter radii of $^{32-35}$Mg, R. Kanungo, A. Prochazka, W. Horiuchi, C. Nociforo, T. Aumann, D. Boutin, D. Cortina-Gil, B. Davids, M. Diakaki, F. Farinon, H. Geissel, R. Gernhäuser, J. Gerl, R. Janik, B. Jonson, B. Kindler, R. Knöbel, R. Krücken, M. Lantz, H. Lenske, Y. Litvinov, B. Lommel, K. Mahata, P. Maierbeck, A. Musumarra, T. Nilsson, C. Perro, C. Scheidenberger, B. Sitar, P. Strmen, B. Sun, Y. Suzuki, I. Szarka, I. Tanihata, Y. Utsuno, H. Weick, and M. Winkler, *Phys. Rev. C* **83**, 021302(R)-1-021302(R)-4 (2011).
21) Nuclear-charge polarization at scission in proton-induced fission of ^{233}U, I. Nishinaka, M. Tanikawa, Y. Nagame, and H. Nakahara, *Eur. Phys. J. A* **47**, 9-1-9-8 (2011).
22) JENDL-4.0: A New Library for Nuclear Science and Engineering, K. Shibata, O. Iwamoto, T. Nakagawa, N. Iwamoto, A. Ichibhara, S. Kunieda, S. Chiba, K. Furutaka, N. Otsuka, T. Ohsawa, T. Murata, H. Matsunobu, A. Zukeran, S. Kamada, and J. Katakura, *J. Nucl. Sci. Tech.* **48**, 1-30 (2011).
23) Neutron one-quasiparticle states in ^{251}Fm$_{151}$ populated via the a decay of ^{255}No, M. Asai, K. Tsukada, H. Haba, Y. Ishii, T. Ichikawa, A. Toyoshima, T. Ishii, Y. Nagame, I. Nishinaka, Y. Kojima, and K. Sueki, *Phys. Rev. C* **83**, 014315-1-014315-15 (2011).

Books & Reviews
1) Symmetry energy and Wigner energy in the mass of nuclei, H. Koura, *Genshikaku-Kenkyu* **55**, 53-63 (2010) (*in Japanese*).
2) Effect of the orientation of projectile nuclei on the synthesis of superheavy elements, K. Nishio, *Nuclear Data News* **98**, 34-43 (2011) (*in Japanese*).

Invited Talks
1) Shell-model approach to exotic nuclei—description by monopole-based universal interaction and development of a new MCSM code, Y. Utsuno, *ECT* Workshop "Reactions and Nucleon Properties in Rare Isotopes,"* Trento, Italy (2010).
2) Multiplicity and energy of neutrons from ^{253}U(n$_{th}$,f) fission fragments, K. Nishio, *Workshop of the Espace de Structure Nucleaire Theorique, The scission process : the last stage of nuclear fission*, Cedex, France (2010).
3) Nuclear Physics Contributions to Nuclear Energy, S. Chiba, *CNS-EFES10 (The 9th CNS-EFES International Summer School)*, Wako, Japan (2010).
4) Effects of nuclear orientation on fusion and fission process for reactions using ^{238}U target nucleus, K. Nishio, *The 24th International Nuclear Physics Conference 2010*, Vancouver, Canada (2010).
5) Fission dynamics in heavy ion collisions on ^{238}U, K Nishio, *Scientific Workshop on Nuclear Fission and Dynamics and the Emission of Prompt Neutrons and Gamma Rays*, Sinaia, Romania (2010).
6) Study for fusion-fission and quasifission in reactions using ^{238}U target nucleus, K. Nishio, *International Symposium on Quasifission Process in Heavy Ion Reactions*, Messina, Italy (2010).
7) Towards petascale nuclear-structure calculation: shell-model case, Y. Utsuno, *French-Japanese Symposium on Nuclear Structure Problems*, Wako, Japan (2011).

Research Group for Superheavy Elements

Papers
1) Extraction Chromatographic Behavior of Rf, Zr, and Hf in HCl Solution with Styrene-divinylbenzene Copolymer Resin Modified by TOPO (Trioctylphosphine Oxide), A. Toyoshima, Y. Kasamatsu, K. Tsukada, M. Asai, Y. Ishii, H. Toume, I. Nishinaka, T. K. Sato, Y. Nagame, M. Schädel, H. Haba, S. Goto, H. Kudo, K. Akiyama, Y. Oura, K. Ooe, A. Shinohara, K. Sueki, and J. V. Kratz, *J. Nucl. Radiochem. Sci.* **11**, 7-11 (2010).
2) Ion-exchange behavior of Zr and Hf as homologues of element 104, Rf, in H_2SO_4 and H_2SO_4 /$HClO_4$ mixed solutions, Z. J. Li, A. Toyoshima, K. Tsukada, and Y. Nagame, *Radiochim. Acta* **98**, 7-12 (2010)
3) In-beam γ-ray spectroscopy of ^{248,250,252}Cf by neutron-transfer reactions using a Cf target, R. Takahashi, T. Ishii, M. Asai, D. Nagae, H. Makii, K. Tsukada, A. Toyoshima, Y. Ishii, M. Matuda, A. Makishima, T. Shizuma, T. Kohno, and M. Ogawa, *Phys. Rev. C* **81**, 057303-1-057303-4 (2010).
4) Nuclear orientation in the reaction ^{34}S + ^{238}U and synthesis of the new isotope ^{268}H, K. Nishio, S. Hofmann, F. P. Hessberger, D. Ackermann, S. Antalic, Y. Aritomo, V. F. Comas, Ch. E. Düllmann, A. Gorshkov, R. Graeger, K. Hagino, S. Heinz, J. A. Heredia, K. Hirose, H. Ikezoe, J. Khuyagbaatar, B. Kindler, I. Kojouharov, B. Lommel, R. Mann, S. Mitsuoka, Y. Nagame, I. Nishinaka, T. Ohtsuki, A. G. Popeko, S. Saro, M. Schädel, A. Türler, Y. Watanabe, A. Yakushev, and A. V. Yeremin, *Phys. Rev. C* **82**, 024611-1-024611-9 (2010).
5) Neutron one-quasiparticle states in ^{251}Fm$_{151}$ populated via the α decay of ^{255}No, M. Asai, K. Tsukada, H. Haba, Y. Ishii, T. Ichikawa, A. Toyoshima, T. Ishii, Y. Nagame, I. Nishinaka, Y. Kojima, and K. Sueki, *Phys. Rev. C* **83**, 014315-1-014315-12 (2011)
6) Nuclear-charge polarization at scission in proton-induced fission of ^{233}U, I. Nishinaka, M. Tanikawa, Y. Nagame, and H. Nakahara, *Eur. Phys. J. A* **47**, 9-1-9-8 (2011).

Invited Talks
1) Strategy for approaching superheavy-nucleus spectroscopy, M. Asai, *2010 Autumn Meeting of the Physical Society of Japan*, Kitakyushu, Japan (2010).
2) Chemistry of superheavy elements – Experimental achievements and perspectives, M. Schädel, *The 54th Symposium on Radiochemistry*, Suita, Japan (2010).
3) The Recent Superheavy Element Chemistry at JAEA, Y. Nagame, *The 2nd Int. Conf. on Appli. of Radiotracers in Chem., Envi. and Bio. Sci.*, Kolkata, India (2010).
4) Chemistry of superheavy elements: Experimental achievements and perspectives, M. Schädel, *Pacifichem 2010*, Honolulu, USA (2010).
5) Electrochemistry of the heaviest elements, A. Toyoshima, *Pacifichem 2010*, Honolulu, USA (2010).

Research Group for Actinide Materials Science

Papers
1) Anisotropic Spin Fluctuations in Heavy-Fermion Superconductor $NpPd_5Al_2$, H. Chudo, H. Sakai, Y. Tokunaga, S. Kambe, D. Aoki, Y. Homma, Y. Haga, T. D. Matsuda, Y. Ōnuki and H. Yasuoka, *J. Phys. Soc. Jpn.* **79**, 053704-1-053704-4 (2010).
2) Angle Resolved Photoemission Study on Uranium Compounds, S.-i. Fujimori, T. Ohkochi, T. Okane, Y. Saitoh, A. Fujimori, H. Yamagami, Y. Haga, E. Yamamoto and Y. Ōnuki, *IOP Conf. Ser.: Mater. Sci. Eng.* **9**, 012045-1-012045-8 (2010).
3) Magnetism and Superconductivity in the new Family of Actinide Compounds: $AnPd_5Al_2$, Y. Haga, Y. Homma, D. Aoki, S. Ikeda, T. D. Matsuda, N. Tateiwa, E. Yamamoto, A. Nakamura, K. Nakajima, Y. Arai, F. Honda, R. Settai and Y. Ōnuki, *IOP Conf. Ser.: Mater. Sci. Eng.* **9**, 012046-1-012046-7 (2010).
4) Similarity of the Fermi Surface in the Hidden Order State and in the Antiferromagnetic State of URu_2Si_2, E. Hassinger, G. Knebel, T. D. Matsuda, D. Aoki, V. Taufour, and J. Flouquet, *Phys. Rev. Lett.* **105**, 216409-1-216409-4 (2010).
5) Fermi Surface Properties of Paramagnetic $NpCd_{11}$ with a Large Unit Cell, Y. Homma, D. Aoki, Y. Haga, R. Settai, H. Sakai, S. Ikeda, E. Yamamoto, A. Nakamura, Y. Shiokawa, T. Takeuchi, H. Yamagami, and Y. Ōnuki, *IOP Conf. Ser.: Mater. Sci. Eng.* **9**, 012091-1-012091-8 (2010).
6) One-Component Description of Magnetic Excitations in the Heavy-Fermion Compound $CeIrIn_5$, S. Kambe, Y. Tokunaga, H. Sakai, H. Chudo, Y. Haga, T. D. Matsuda, and R.E. Walstedt, *Phys. Rev. B* **81**, 140405(R)-1-140405(R)-4 (2010).
7) Molecular and Crystal Structures of Plutonyl(VI) Nitrate Complexes with N-Alkylated 2-Pyrrolidone Derivatives: Cocrystallization Potentiality of U^{VI} and Pu^{VI}, S.-Y. Kim, K. Takao, Y. Haga, E. Yamamoto, Y. Kawata, Y. Morita, K. Nishimura, and Y. Ikeda, *Crystal Growth & Design* **10**, 2033-2036 (2010).
8) Fermi Surface Properties of Ferromagnet UCu_2Si_2, T. D. Matsuda, S. Ikeda, E. Yamamoto, Y. Haga, H. Shishido, H. Yamagami, R. Settai, and Y. Ōnuki, *J. Phys. Soc. Jpn.* **79**, 114712-1-114712-4 (2010).

9) Neutron Scattering Study on U-Dichalcogenides, N. Metoki, K. Kaneko, S. Ikeda, H. Sakai, E. Yamamoto, Y. Haga, Y. Homma, and Y. Shiokawa, *IOP Conf. Ser.: Mater. Sci. Eng.* **9**, 012088-1-012088-8 (2010).
10) New Defect-Crystal-Chemical Approach to non-Vegardianity and Complex Defect Structure of Fluorite-Based MO_2–$LnO_{1.5}$ Solid Solutions (M^{4+} = Ce, Th; Ln^{3+} = Lanthanide) Part II: Detailed Local-Structure and Ionic-Conductivity Analysis, A. Nakamura, *Solid State Ionics* **181**, 1631-1653 (2010).
11) New Defect-Crystal-Chemical Approach to non-Vegardianity and Complex Defect Structure of Fluorite-Based MO_2–$LnO_{1.5}$ Solid Solutions (M^{4+} = Ce, Th; Ln^{3+} = Lanthanide) Part I: Model Description and Lattice-Parameter Data Analysis, A. Nakamura, *Solid State Ionics* **181**, 1543-1564 (2010).
12) Anomalous Temperature Dependence of Lower Critical Field in Ultraclean URu_2Si_2, R. Okazaki, M. Shimozawa, H. Shishido, M. Konczykowski, Y. Haga, T. D. Matsuda, E. Yamamoto, Y. Ōnuki, Y. Yanase, T. Shibauchi and Y. Matsuda, *J. Phys. Soc. Jpn.* **79**, 084705-1-084705-7 (2010).
13) *5f*-electronic States of Neptunium Compounds: $NpGe_3$, $NpRhGa_5$ and $NpCd_{11}$, Y. Ōnuki, D. Aoki, Y. Homma, Y. Haga, S. Yoshiuchi, R. Settai, H. Sakai, S. Ikeda, E. Yamamoto, A. Nakamura, Y. Shiokawa, T. Takeuchi, and H. Yamagami, *IOP Conf. Ser.: Mater. Sci. Eng.* **9**, 012089-1-012089-8 (2010).
14) Heavy Fermion State and Quantum Criticality, Y. Ōnuki, R. Settai, F. Honda, N. D. Dung, T. Ishikura, T. Takeuchi, T. D. Matsuda, N. Tateiwa, A. Nakamura, E. Yamamoto, Y. Haga, D. Aoki, Y. Homma, H. Harima, and H. Yamagami, *Physica B* **405**, 2194-2199 (2010).
15) Crystal Structure and Physical Properties of Uranium-Copper Oxyphosphide UCuPO, H. Sakai, N. Tateiwa, T.D. Matsuda, T. Sugai, E. Yamamoto, and Y. Haga, *J. Phys. Soc. Jpn.* **79**, 074721-1-074721-5 (2010).
16) New Surprises "Down Below": Recent Successes in the Synthesis of Actinide Materials, J. L. Sarrao, Y. Haga, and R. C. C. Ward, *MRS Bulletin* **35**, 877-882 (2010).
17) Metamagnetic Behavior in Heavy-Fermion Compound $YbIr_2Zn_{20}$, T. Takeuchi, S. Yasui, M. Toda, M. Matsushita, S. Yoshiuchi, M. Ohya, K. Katayama, Y. Hirose, N. Yoshitani, F. Honda, K. Sugiyama, M. Hagiwara, K. Kindo, E. Yamamoto, Y. Haga, T. Tanaka, Y. Kubo, R. Settai and Y. Ōnuki, *J. Phys. Soc. Jpn.* **79**, 064609-1-064609-15 (2010).
18) Appropriate Pressure-Transmitting Media for Cryogenic Experiment in the Diamond Anvil Cell Up to 10 GPa, N. Tateiwa and Y. Haga, *J. Phys.: Conf. Ser.* **215**, 01278-1-01278-8 (2010).
19) Signature of Hidden Order and Evidence for Periodicity Modification in URu_2Si_2, R. Yoshida, Y. Nakamura, M. Fukui, Y. Haga, E. Yamamoto, Y. Ōnuki, M. Okawa, S. Shin, M. Hirai, Y. Muraoka and T. Yokoya, *Phys. Rev. B* **82**, 205108-1-205108-6 (2010).
20) Low-Temperature Magnetic Orderings and Fermi Surface Properties of $LaCd_{11}$, $CeCd_{11}$, and $PrCd_{11}$ with a Caged Crystal Structure, S. Yoshiuchi, T. Takeuchi, M. Ohya, K. Katayama, M. Matsushita, N. Yoshitani, N. Nishimura, H. Ota, N. Tateiwa, E. Yamamoto, Y. Haga, H. Yamagami, F. Honda, R. Settai, and Y. Ōnuki, *J. Phys. Soc. Jpn.* **79**, 044601-1-044601-11 (2010).
21) Muon knight shift measurements in $CeCoIn_5$ below 17 kOe, W. Higemoto, A. Koda , R. Kadono, K. Ohishi, Y. Haga, H. Shishido, R. Settai, and Y. Ōnuki, *J. Phys.: Conf. Ser.* **225**, 012013-1-012013-5 (2010).
22) First Observation of Quantum Oscillations in the Ferromagnetic Superconductor UCoGe, D. Aoki, I. Sheikin, T. D. Matsuda, V. Taufour, G. Knebel, and J. Flouquet, *J. Phys. Soc. Jpn.* **80**, 013705-1-013705-4 (2011).
23) Trends in Heavy Fermion Matter, J. Flouquet, D. Aoki, F. Bourdarot, F. Hardy, E. Hassinger, G. Knebel, T. D. Matsuda, C. Meingast, C. Paulsen, and V. Taufour, *J. Phys.: Conf. Ser.* **273**, 012001-1-012001-25 (2011).
24) Inelastic Contribution of the Resistivity in the Hidden Order in URu_2Si_2, E. Hassinger, T. D. Matsuda, G. Knebel, V. Taufour, D. Aoki, and J. Flouquet, *J. Phys.: Conf. Ser.* **273**, 012031-1-012031-4 (2011).
25) Magnetic and Superconducting Properties of $CeRhGe_2$ and $CePtSi_2$, Y. Hirose, N. Nishimura, F. Honda, K. Sugiyama, M. Hagiwara, K. Kindo, T. Takeuchi, E. Yamamoto, Y. Haga, M. Matsuura, K. Hirota, A. Yasui, H. Yamagami, R. Settai, and Y. Ōnuki, *J. Phys. Soc. Jpn.* **80**, 024711-1-024711-12 (2011).
26) Incommensurate-to-Commensurate Magnetic Phase Transition in $SmIn_3$ Observed by Muon Spin Relaxation, T. U. Ito, W. Higemoto, K. Ninomiya, H. Luetkens, T. Sugai, Y. Haga, and H.S. Suzuki, *J. Phys. Soc. Jpn.* **80**, 033710-1-033710-4 (2011).
27) Electronic structure of URu_2Si_2 in paramagnetic phase studied by soft x-ray photoemission spectroscopy, I. Kawasaki, S.-i. Fujimori, Y. Takeda, T. Okane, A. Yasui, Y. Saitoh, H. Yamagami, Y. Haga, E. Yamamoto, and Y. Ōnuki, *J. Phys.: Conf. Ser.* **273**, 012039-1-012039-4 (2011).
28) Magnetic Anisotropy and Spin-Glass Behavior in Single Crystalline U_2PdSi_3, D. X. Li, A. Kimura, Y. Haga, S. Nimori and T. Shikama, *J. Phys.: Condens. Matter* **23**, 076003-1-076003-7 (2011).
29) Anomalous Low-Field Diamagnetic Response in Ultraclean URu_2Si_2 Superconductor, R. Okazaki, M. Shimozawa, H. Shishido, M. Konczykowski, Y. Haga, T. D. Matsuda, E. Yamamoto, Y. Ōnuki, Y. Yanase, T. Shibauchi and Y. Matsuda, *J. Phys.: Conf. Ser.* **273**, 012081-1-012081-4 (2011).
30) Rotational Symmetry Breaking in the Hidden-Order Phase of URu_2Si_2, R. Okazaki, T. Shibauchi, H. J. Shi, Y. Haga, T. D. Matsuda, E. Yamamoto, Y. Ōnuki, H. Ikeda and Y. Matsuda, *Science* **331**, 439-442 (2011).
31) Relation between Metamagnetic Transition and Quantum Critical Point in Heavy Fermion Compound $YbIr_2Zn_{20}$, Y. Ōnuki, S. Yasui, S. Yoshiuchi, M. Ohya, M. Matsushita, Y. Hirose, T. Takeuchi, F. Honda, R. Settai, K. Sugiyama, E. Yamamoto and Y. Haga, *J. Phys.: Conf. Ser.* **273**, 012013-1-012013-4 (2011).
32) Magnetization in the Superconducting Mixed State of the Heavy-Fermion Compound UBe_{13}, Y. Shimizu, Y. Ikeda, T. Wakabayashi, K. Tenya, Y. Haga, H. Hidaka, T. Yanagisawa and H. Amitsuka, *J. Phys.: Conf. Ser.* **273**, 012084-1-012084-4 (2011).
33) Single Crystal Growth and Physical Properties of Ternary Uranium Compounds UM^2Al_{10} (M =Fe, Ru and Os), T. Sugai, Y. Haga, T. D. Matsuda, E. Yamamoto, N. Tateiwa, F. Honda, R. Settai and Y. Ōnuki, *J. Phys.: Conf. Ser.* **273**, 012122-1-012122-4 (2011).
34) High-Pressure Electrical Resistivity Measurement on Heavy Fermion Superconductor URu_2Si_2 Using Super Clean Crystal, N. Tateiwa, T. D. Matsuda, Y. Haga, E. Yamamoto and Y. Ōnuki, *J. Phys.: Conf. Ser.* **273**, 012087-1-012087-4 (2011).
35) Magnetic Field and Pressure Phase Diagrams of Uranium Heavy-Fermion Compound U_2Zn_{17}, N. Tateiwa, S. Ikeda, Y. Haga, T. D. Matsuda, E. Yamamoto, K. Sugiyama, M. Hagiwara, K. Kindo and Y. Ōnuki, *J. Phys. Soc. Jpn.* **80**, 014706-1-014706-8 (2011).
36) Soft X-Ray Angle-Resolved Photoemission Study of $YbCu_2Ge_2$, A. Yasui, S.-I. Fujimori, I. Kawasaki, T. Okane, Y. Takeda, Y. Saitoh, H. Yamagami, A. Sekiyama, R. Settai, T. D. Matsuda, Y. Haga and Y. Ōnuki, *J. Phys.: Conf. Ser.* **273**, 012067-1-012067-4 (2011).
37) Electronic Structure of $U(Ru_{1-x}Rh_x)_2Si_2$ Studied by Laser Angle-Resolved Photoemission Spectroscopy, R. Yoshida, Y. Nakamura, M. Fukui, Y. Haga, E. Yamamoto, Y. Ōnuki, M. Okawa, S. Shin, M. Hirai, Y. Muraoka and T. Yokoya, *J. Phys.: Conf. Ser.* **273**, 012021-1-012021-4 (2011).

Books & Reviews

1) Evaluation of Pressure-transmitting Media for Cryogenic Experiment under High Pressure, N. Tateiwa, Y. Haga, *KOTAI BUTSURI* **45**, 225-233 (2010) (*in Japanese*).

Invited Talks

1) New compounds in actinide-based intermetallic system and physical properties, Y. Haga, *The Third International Workshop on Dual Nature of f-Electrons*, Dresden, Germany (2010).
2) Unconventional magnetism and superconductivity in the ternary actinide compounds $AnPd_5Al_2$, Y. Haga, Y. Homma, D. Aoki, T. D. Matsuda, N. Tateiwa, H. Sakai, S. Yoshio, T. Sugai, A. Nakamura, E. Yamamoto, Y. Ōnuki, *International Conference on Strongly Correlated Electron Systems*, Santa Fe, USA (2010).
3) Thermodynamic study on anomalous magnetism and superconductivity in actinide compounds, Y. Haga, *The North American Calorimetry Conference*, Colorado Springs, USA (2010).
4) New Defect-Crystal-Chemistry Model for Non-Vegardianity and Non-Random Defect Structure of Defect-Fluorite MO_2–$LnO_{1.5}$ Solid Solutions (M^{4+} = Ce, Th; Ln^{3+} = Lanthanide), A. Nakamura, *21st IUPAC International Conference on Chemical Thermodynamics (ICCT-2010)*, Tsukuba, Ibaraki (2010).
5) New Defect-Crystal-Chemical Approach to non-Vegardianity and Complex Defect Structure of Fluorite-Based MO_2–$LnO_{1.5}$ Solid Solutions (M^{4+} = Ce, Th; Ln^{3+} = Lanthanide), A. Nakamura, *3rd International Symposium on Materials Chemistry (ISMC-2010)*, Mumbai, India (2010).
6) Single crystal growth of strongly correlated uranium and transuranium compounds, Y. Haga, *The 1st ASRC International Workshop: New Approach to the Exotic Phases of Actinides Compounds under Unconventional Experimental Conditions*, Sakai, Japan (2011).
7) High-pressure studies on actinide compound in Tokai, N. Tateiwa, *The 1st ASRC International Workshop: New Approach to the Exotic Phases of Actinides Compounds under Unconventional Experimental Conditions*, Tokai, Japan (2011).

Research Group for Condensed Matter Physics of Heavy Element Systems

Papers

1) ^{59}Co NMR Shift Anomalies and Spin Dynamics in the Normal State of Superconducting $CeCoIn_5$, Verification of Two-Dimensional Antiferromagnetic Spin Fluctuations, H. Sakai, S. -H. Baek, S. E. Brown, F. Ronning, E. D. Bauer, and J. D. Thompson, *Phys. Rev. B* **82**, 020501(R)-1-0205501(R)-4 (2010).
2) Crystal Structure and Physical Properties of Uranium–Copper Oxyphosphide UCuPO, H. Sakai, N. Tateiwa, T. D. Matsuda, T. Sugai, E. Yamamoto, and Y. Haga, *J. Phys. Soc. Jpn.* **79**, 074721-1-074721-5 (2010).
3) Anisotropic Spin Fluctuations and Superconductivity in "115" Heavy Fermion Compounds: ^{59}Co NMR Study in $PuCoGa_5$, S. -H. Baek, H. Sakai, E. D. Bauer, J. N. Mitchell, J. A. Kennison, F. Ronning and J. D. Thompson, *Phys. Rev. Lett.* **105**, 217002-1-217002-4 (2010).
4) Crystal-Electric-Field Effects and Quadrupole Fluctuations in $Ce_3Au_3Sb_4$ Detected by Sb NQR, S. -H. Baek, H. Sakai, H. Lee, Z. Fisk, E. D. Bauer, and J. D. Thompson, *Phys. Rev. B* **82**, 035203-1-035203-4 (2010).
5) La substitution effect and hyperfine-enhanced ^{141}Pr nuclear spin dynamics in $PrPb_3$, ^{139}La NMR study in $Pr_{0.97}La_{0.03}Pb_3$, Y. Tokunaga, H. Sakai, H. Chudo, S. Kambe, H. Yasuoka, H. S. Suzuki, R. E. Walstedt, Y. Homma, D. Aoki, and Y. Shiokawa, *Phys. Rev. B* **82**, 104401-1-104401-6 (2010).
6) NMR Evidence for the 8.5 K Phase transition in Americium dioxide, Y. Tokunaga, T. Nishi, S. Kambe, M. Nakada, A. Itoh, Y. Homma, H. Sakai, and H. Chudo, *J. Phys. Soc. Jpn.* **79**, 053705-1-053705-4 (2010).
7) Anisotropic spin fluctuations in Heavy-fermion superconductor $NpPd_5Al_2$, H. Chudo, H. Sakai, Y.Tokunaga, S. Kambe, D. Aoki, Y.Homma, Y. Haga, T. D. Matsuda, Y. Ōnuki, and H. Yasuoka, *J. Phys. Soc. Jpn.* **79**, 053704-1-053704-4 (2010).
8) Evidence for appearance of an internal field in the ordered state of $CeRu_2Al_{10}$ by μ^+SR: S. Kambe, H. Chudo, Y. Tokunaga, T. Koyama, H. Sakai, T. U. Ito, N. Kazuhiko, W. Higemoto, T. Takesaka, T. Nishioka and Y. Miyake, *J. Phys. Soc. Jpn.* **79**, 053708-1-053708-4 (2010).
9) ^{27}Al-NQR/NMR Study of Kondo Semiconductor $CeFe_2Al_{10}$, Y. Kawamura, S. Edamoto, T. Takesaka, T. Nishioka, H. Kato, M. Matsumura, Y. Tokunaga, S. Kambe, and H. Yasuoka, *J. Phys. Soc. Jpn.* **79**, 103701-1-103701-4 (2010).
10) Energy scale of the electron-boson spectral function and superconductivity in $NpPd_5Al_2$, G. A. Ummarino, R. Caciuffo, H. Chudo, and S. Kambe, *Phys Rev. B* **82**, 104510-1-104510-7 (2010).
11) Quantum critical behavior in heavy fermion superconductor $CeIrIn_5$, S. Kambe, H. Sakai, Y. Tokunaga, and R.E. Walstedt, *Phys Rev. B***82**, 144503-1-144503-7 (2010).
12) One-component description for magnetic excitations in heavy fermion $CeIrIn_5$, S. Kambe, Y. Tokunaga, H. Sakai, H. Chudo, Y. Haga, T. D. Matsuda, and R. E. Walstedt, *Phys. Rev. B* **81**, 140405(R)-1-140405(R)-4 (2010).
13) Incommensurate-to-Commensurate Magnetic Phase Transition in $SmIn_3$ Observed by Muon Spin Relaxation, T. U. Ito, W. Higemoto, K. Ninomiya, H. Luetkens, T. Sugai, Y. Haga, and H. S. Suzuki, *J. Phys. Soc. Jpn.* **80**, 033710-1-033710-4 (2011).
14) Suppression of time-reversal symmetry breaking superconductivity in $Pr(Os_{1-x}Ru_x)_4Sb_{12}$ and $Pr_{1-y}La_yOs_4Sb_{12}$, Lei Shu, W. Higemoto, Y. Aoki, A. D. Hillier, K. Ohishi, K. Ishida, R. Kadono, A. Koda, O. O. Bernal, D. E. MacLaughlin, Y. Tunashima, Y. Yonezawa, S. Sanada, D. Kikuchi, H. Sato, H. Sugawara, T. U. Ito, and M. B. Maple, *Phys. Rev. B* **83**, 100504(R)-1-100504(R)-4 (2011).
15) Microscopic study of antiferromagnetic ground state and possible high-field ordered state in $CeOs_4Sb_{12}$ using muon spin rotation and relaxation, T. U. Ito, W. Higemoto, K. Ohishi, K. Satoh, Y. Aoki, S. Toda, D. Kikuchi, H. Sato, and C. Baines, *Phys. Rev. B* **82**, 014420-1-014420-8 (2010).
16) Quasiparticle excitations in newly discovered antiperovskite superconductor $ZnNNi_3$, K. Ohishi, T. U. Ito, W. Higemoto, T. Yamazaki, A. Uehara, K. Kozawa, Y. Kimishima and M. Uehara, *Physica C* **470** Suppl. 1, S705-S706 (2010).
17) μ^+ diffusion in cubic *f*-electron compounds observed by high transverse field μ^+SR, T. U. Ito, W. Higemoto, K. Ohishi, N. Nishida, R. H. Heffner, Y. Aoki, H. S. Suzuki, T. Onimaru, H. Tanida, and S. Takagi, *J. Phys.: Conf. Ser.* **225**, 012021-1-012021-4 (2010).
18) The EPICS-based remote control system for muon beam line devices at J-PARC MUSE, T. U. Ito, K. Nakahara, M. Kawase, H. Fujimori, Y. Kobayashi, W. Higemoto, and Y. Miyake, *J. Phys.: Conf.* **225**, 012022-1-012022-4 (2010).
19) μSR study of $CeRhIn_5$ under applied pressure, R.H. Heffner, T. Goko, D. Andreica, K. Ohishi, W. Higemoto, T. U. Ito, A. Amato, J. Spehling, H. –H. Klauss, E. D. Bauer, J. D. Thompson, and Y. J. Uemura, *J. Phys.: Conf.* **225**, 012011-1-012011-4 (2010).
20) Magnetism in $Ce_2Rh(In,Sn)_8$ heavy-fermion compound, Kazuki Ohishi, Takao Suzuki, Robert H. Heffner, Takashi U. Ito, Wataru Higemoto, and Eric D. Bauer, *J. Phys.: Conf.* **225**, 012042-1-012042-4 (2010).
21) JAEA-ASRC muon research at J-PARC MUSE, W. Higemoto, T. U. Ito, K. Ninomiya, R. H. Heffner, K. Shimomura, K. Nishiyama, and Y. Miyake, *J. Phys.: Conf.* **225**, 012012-1-012012-4 (2010).
22) J-PARC Muon Facility, MUSE, Y. Miyake, K. Shimomura, N. Kawamura, P. Strasser, S. Makimura, A. Koda, H. Fujimori, K. Nakahara, S. Takeshita, Y. Kobayashi, K. Nishiyama, W. Higemoto, T. U. Ito, K. Ninomiya, M. Kato, R. Kadono, N. Sato, and K. Nagamine, *J. Phys.: Conf.* **225**, 012036-1-012036-4 (2010).
23) J-PARC Decay Muon Channel Construction Status, P. Strasser, K. Shimomura, A. Koda, N. Kawamura, H. Fujimori, S. Makimura, Y. Kobayashi, K. Nakahara, M. Kato, S. Takeshita, M. Hiraishi, M. Miyazaki, W. Higemoto, T. U. Ito, K. Ninomiya, K. Ishida, M. K. Kubo, R. Kadono, K. Nishiyama, and Y. Miyake, *J. Phys.: Conf.* **225**, 012050-1-012050-4 (2010).
24) Development of elemental analysis by muonic X-ray measurement in J-PARC, K. Ninomiya, T. Nagatomo, K. M. Kubo, P. Strasser, N. Kawamura, K. Shimomura, Y. Miyake, T. Saito and W. Higemoto, *J. Phys.: Conf.* **225**, 012040-1-012040-4 (2010).
25) Muon Knight shift measurements in $CeCoIn_5$ below 17 kOe, W. Higemoto, A. Koda, R. Kadono, K. Ohishi, Y. Haga, H. Shishido, R. Settai, and Y. Ōnuki, *J. Phys.: Conf.* **225**, 012013-1-012013-4 (2010).
26) Neutron scattering study on U-dichalcogenides, N. Metoki, K. Kaneko, S. Ikeda, H. Sakai, E. Yamamoto, Y. Haga, Y. Homma, and Y. Shiokawa, *IOP Conf. Series: Materials Science and Engineering* **9**, 012088-1-012088-8 (2010).
27) *5f*-electronic states of neptunium compounds: $NpGe_3$, $NpRhGa_5$ and $NpCd_{11}$, Y. Ōnuki, D. Aoki, Y. Homma, Y. Haga, S. Yoshiuchi, R. Settai, H. Sakai, S. Ikeda, E. Yamamoto, A. Nakamura, Y. Shiokawa, T. Takeuchi, and H. Yamagami, *IOP Conf. Series: Materials Science and Engineering* **9**, 012089-1- 012089-8 (2010).
28) Fermi surface properties of paramagnetic $NpCd_{11}$ with a large unit cell, Y. Homma, D. Aoki, Y. Haga, R. Settai, H. Sakai, S. Ikeda, E. Yamamoto, A. Nakamura, Y. Shiokawa, T. Takeuchi, H. Yamagami, and Y. Ōnuki, *IOP Conf. Series: Materials Science and Engineering* **9**, 012091-1-012091-8 (2010).

Invited talks

1) Anisotropy of antiferromagnetic spin fluctuations in the heavy fermion superconductors of CeM^1In_5 and PuM^2Ga_5 (M=Co, Rh), H. Sakai, *MRS Spring Meeting*, San Francisco, USA (2010).
2) NMR Studies of Transuranium Dioxides, Yo Tokunaga, *Plutonium Futures- The Science 2010*, Keystone, USA (2010).
3) NMR study of exotic magnetism and superconductivity in actinide compounds, *EURACT-NMR*, S. Kambe, Karlsruhe, Germany (2010).
4) Coherence between localized and itinerant excitations in heavy fermion $CeIrIn_5$, *Dual Nature of f-electrons*, S. Kambe, Dresden, Germany (2010).
5) Spin dynamics in Heavy Fermion systems, S. Kambe, *On the Heavy fermion Road*, Paris, France (2010).
6) Magnetic fluctuations and Unconventional superconductivity in Actinide compounds International conference, S. Kambe, *Plutonium Futures- The Science 2010*, Keystone, USA (2010).
7) Strong electron correlations in Actinide compounds, S. Kambe, *International workshop "Novel Phenomena in Solid state and Life Science"*, Kyoto, Japan (2010).
8) Clarification of exotic properties in *f*-electron systems, S. Kambe, *Spinics research meeting*, Hitachi, Japan (2010).
9) Material science by μSR in J-PARC, W. Higemoto, *Research meeting of Physics and Chemistry*, Hiroshima, Japan (2010).
10) Our Recent Progress of NMR Measurements Under High Pressures in Our Research Group of ASRC-JAEA, H. Sakai, *The 1st ASRC International Workshop*, Tokai, Japan (2011).
11) NMR studies in actinide oxides and intermetallic compounds, Yo Tokunaga, *The 1st ASRC International Workshop*, Tokai, Japan (2011).
12) NMR studies in Actinide Dioxides, Yo Tokunaga, *Actinide XAS 2011*, Harima, Japan (2011).
13) NMR of multipolar ordering, Yo Tokunaga, *Meeting of Physical society of Japan*, Niigata, Japan (2011).

Research Group for Hadron Physics

Papers

1) Enhanced Production of Direct Photons in Au + Au Collisions at $(s_{NN})^{1/2}$ = 200 GeV and Implications for the Initial Temperature, A. Adare, K. Imai, S. Sato, K. Tanida, *et al., Phys. Rev. Lett.* **104**, 13231-1-13231-6 (2010).
2) Near Threshold L(1520) Production by the $\gamma p \rightarrow K^+\Lambda(1520)$ Reaction at Forward K^+ Angles, H. Kohri, K. Imai, *et al., Phys. Rev. Lett.* **104**, 172001-1-172001-5 (2010).
3) Measurement of Spin-Density Matrix Elements for ϕ-Meson Photoproduction from Protons and Deuterons Near Threshold, W. C. Chang, K. Imai, *et al., Phys. Rev.* C **82**, 015205-1-015205-25 (2010).
4) Transverse momentum dependence of η meson suppression in Au+Au collisions at $(s_{NN})^{1/2}$ = 200 GeV, A. Adare, K. Imai, K. Tanida, *et al., Phys. Rev.* **C82**, 011902-1-011902-7 (2010).
5) Transition in Yield and Azimuthal Shape modification in Dihadron Correlations in relativistic Heavy Ion Collisions, A. Adare, K. Imai, K. Tanida, *et al., Phys. Rev. Lett.* **104**, 252301-1-252301-7 (2010).
6) Transverse momentum dependence of J/ψ polarization at midrapidity in *p*+*p* collisions at $s^{1/2}$ = 200 GeV, A. Adare, K. Imai, K. Tanida, *et al. Phys. Rev.* D **82**, 012001-1-012001-17 (2010).
7) Measurement of transverse single-spin asymmetries for J/ψ polarization in polarized *p*+*p* collisions at $s^{1/2}$ = 200 GeV, A. Adare, K. Imai, K. Tanida, *et al., Phys. Rev.* D **82**, 112008-1-112008-13 (2010).
8) The HypHI Phase 0 experiment, T.R. Saito, H. Sugimura, *et al., Nucl. Phys.* A **835**, 110-116 (2010).
9) Elliptic and Hexadecapole flow of Charged Hadrons in Au + Au Collisions at $(s_{NN})^{1/2}$ = 200 GeV, A. Adare, K. Imai, K. Tanida, *et al., Phys. Rev. Lett.* **105**, 062301-1-062301-6 (2010).
10) Azimuthal anisotropy of neutral pion production in Au+Au collisions at $s^{1/2}$ = 200 GeV: Path-length dependence of jet quenching and the role of initial geometry, A. Adare, K. Imai, K. Tanida, *et al., Phys. Rev. Lett.* **105**, 142301-1-142301-7 (2010).
11) High P_T direct photon and π^0 triggered azimuthal jet correlations and measurement of k_T for isolated direct photons in *p*+*p* collisions at $s^{1/2}$ = 200 GeV, A. Adare, K. Imai, S. Sato K. Tanida, *et al., Phys. Rev.* D **82**, 072001-1-072001-18 (2010).
12) Equation of State of Structured Matter at Finite Temperature, T. Maruyama, N. Yasutake, and T. Tatsumi, Prog. Theor. *Phys. Suppl.***186**, 69-74 (2010).
13) Unified Beam Control System of J-PARC Linac, H. Sako, C. K. Allen, H. Ikeda, and G. Shen, *IEEE Transactions and Nuclear Science* **57**, No. 3, 1528-1535 (2010).
14) Suppression of Beam Loss at the First Arc Section in the J-PARC Linac, H. Sako, and M. Ikegami, *IEEE Transactions and Nuclear Science* **57**, No. 5, 2783-2789 (2010).
15) Effects of the $\Lambda(1405)$ on the Structure of Multi-Antikaonic Nuclei, T. Muto, T. Maruyama, and T. Tatsumi, *Nucl. Phys.* A **835**, 370-373 (2010).
16) Current Status and Performance of the J-PARC Accelerators, H. Sako, *Journal of Power and Energy Systems*, **4**, No. 1, 218-233, (2010).
17) Multi-antikaonic nuclei and kaon condensation in dense matter, T. Muto, T. Maruyama, and T. Tatsumi, *AIP Conf. Proc.* **1269**, 233-238 (2010).
18) Cooling of compact stars with quark-hadron mixed phase in the color superconductive state, T. Noda, M. Hashimoto, N. Yasutake, T. Maruyama, T. Tatsumi, and M. Fujimoto, *AIP Conf. Proc.* **1269**, 384-386 (2010).
19) Quark-hadron mixed phase with hyperons in protoneutron stars, N. Yasutake, T. Maruyama, and T. Tatsumi, *Proc. of Sci.* **NIC XI**, 041-1-041-5 (2010).
20) Signatures of hadron-quark mixed phase in gravitational waves, H. Sotani, N. Yasutake, T. Maruyama, and T. Tatsumi, *Phys. Rev. D* **83**, 024014-1-024014-8 (2011).
21) Nuclear modification factors of ϕ mesons in *d* + Au, Cu + Cu, Au + Au collisions at $(s_{NN})^{1/2}$ = 200 GeV, A. Adare, K. Imai, K. Tanida, *et al., Phys. Rev.* C **83**, 024909-1-024909-10 (2011).
22) Cross section and double helicity asymmetry for η meson and their comparison to π^0 production in *p*+*p* collisions at $s^{1/2}$ = 200 GeV, A. Adare, K. Imai, S. Sato, K. Tanida, *et al., Phys. Rev.* D **83**, 032001-1-032001-11 (2011).
23) Cross Section and Parity-Violating Spin Asymmetries of $W^{+/-}$ Boson Production in Polarized *p*+*p* Collisions at $s^{1/2}$=500 GeV, A. Adare, K. Imai, K. Tanida, *et al., Phys. Rev. Lett.* **106**, 062001-1-062001-6 (2011).

Invited Talks

1) Search for H resonance and other exotics at J-PARC, K. Imai, *YIPQS workshop on Exotics from Heavy Ion Collisions*, Kyoto, Japan (2010).
2) J-PARC and its prospects of nuclear and particle physics, K. Imai, *2nd International Ulaanbaatar Conference on the Nuclear Physics and Applications (UBC2010)*, Ulaanbaatar, Mongolia (2010).
3) Status of J-PARC, Hadron and Particle Physics, S. Sato, *International Conference on the Application of Accelerator in Research and Industry*, Fort Worth, USA, (2010).
4) Nucleons and Nuclear Interactions Studied with Spin and Strangeness, K. Imai, *The Autumn Meeting 2010 of Physical Society of Japan*, Kita Kyushu, Japan (2010).
5) J-PARC Facility and Physics, S. Sato, *6th International Conference on Physics and Astrophysics of Quark Gluon Plasma*, Goa, India (2010).

Research Group for Bioactinide

Papers

1) Effects of citrate, NTA and EDTA on the reduction of U(VI) by *Shewanella putrefaciens*, Y. Suzuki, K. Tanaka, N. Kozai, and T. Ohnuki, *Geomicrobiology J.* **27**, 245-250 (2010).
2) Association of actinides with microorganisms and clay: Implications for radionuclide migration from waste-repository sites, T. Ohnuki, N. Kozai, F. Sakamoto, T. Ozaki, T. Kamiya, Y. Suzuki, and A. J. Francis, *Geomicrobiology J.* **27**, 225-230 (2010).
3) Redox behavior of Ce(IV)/Ce(III) in the presence of nitrilotriacetic acid: A surrogate study for An(IV)/An(III) redox behavior, Y. Suzuki, T. Nankawa, A. J. Francis, and T. Ohnuki, *Radiochimica Acta*, **98**, 397-402(2010).
4) Characterization of secondary arsenic-bearing precipitates formed in the bioleaching of

Publication List

enargite by *Acidithiobacillus ferrooxidans*, K. Sasaki, K. Takatsugi, K. Kaneko, N. Kozai, T. Ohnuki, O. H. Tuovinen, and T. Hirajima, *Hydrometallurgy*, 104, 424-431 (2010).
5) Biological nano-mineralization of Ce phosphate by *Saccharomyces cerevisiae*, Mingyu Jiang, T. Ohnuki, N. Kozai, K. Tanaka, Y. Suzuki, F. Sakamoto, E. Kamiishi, and S. Utsunomiya, *Chemical Geology*, **277**, 61-69 (2010).
6) A specific Ce oxidation process during sorption of rare earth elements on biogenic Mn oxide produced by *Acremonium* sp. strain KR21-2, K. Tanaka, Y. Tani, Y. Takahashi, M. Tanimizu, Y. Suzuki, N. Kazai, and T. Ohnuki, *Geochimica et Cosmochimica Acta*, **74**, 5463-5477 (2010).
7) Flavin mononucleotide mediated electron pathway for microbial U(VI) reduction, Y. Suzuki, Y. Kitatsuji, T. Ohnuki, and S. Tsujimura, *Physical Chemistry Chemical Physics*, **12**, 10081-10087 (2010).

Books & Reviews
1) Effects of Organic Acids on Biotransformation of Acinides, T. Ohnuki, N. Kozai, T. Ozaki, F. Sakamoto, Y. Suzuki, T. Nankawa, and T. Yoshida, in Nuclear Energy and the Environment; edited by Wai, C., Mincher B. J., ACS syposium series 1046, 333-348 (2010).

Invited Talks
1) Mineralization of actinides on the surface of microorganisms and minerals. T. Ohnuki, *Pacifichem 2010*, Honolulu, USA (2010).
2) Mineralization of heavy elements by microorganism, K. Tanaka, *2010 Geochemical Society Annual Meeting*, Kumagai, Japan (2010).

Research Group for Radiation and Biomolecular Science

Papers
1) A novel technique using DNA denaturation to detect multiply induced single-strand breaks in a hydrated plasmid DNA molecule by X-ray and $^4He^{2+}$ ion irradiation, A. Yokoya, N. Shikazono, K. Fujii, M. Noguchi, and A. Urushibara, *Radiat. Protect. Dosim.* **143**, 219-225 (2011).
2) A model for analysis of the yield and the level of clustering of radiation-induced DNA strand breaks in hydrated plasmids, N. Shikazono, A. Yokoya, A. Urushibara, M. Noguchi, and K. Fujii. *Radiat. Protect. Dosim.* **143**, 181-185 (2011).
3) Pulse radiolysis study on free radical scavenger edaravone (3-methyl-1-phenyl-2-pyrazolin-5-one). 2: A comparative study on edaravone derivatives, K. Hata, M.Z. Lin, Y. Katsumura, Y. Muroya, H.Y. Fu, S. Yamashita, and H. Nakagawa, *J. Radiat. Res.* **52**, 15-23 (2011).
4) Fluorescent probe for steady-state radiolysis with heavy ions 1: LET effects and time dependence of OH yields, T. Maeyama, S. Yamashita, G. Baldacchino, M. Taguchi, A. Kimura, Y. Katsumura, and T. Murakami, *Radiat. Phys. Chem.* **80**, 535-539 (2011).
5) Temperature and density effects on the absorption maximum of solvated electrons in sub- and supercritical methanol, 7. Y. Yan, M. Lin, Y. Katsumura, Y. Muroya, S. Yamashita, K. Hata, J. Meesungnoen, J.-P. Jay-Gerin, *Can. J. Chem.* **88**, 1026-1033 (2010).
6) High rate crystallization of polycarbonate in spincast thin film, S. Ata, T. Oka, C. He, T. Ohdaira, R. Suzuki, K. Ito, Y. Kobayashi, and T. Ougizawa, *J. Polym. Sci. Pt. B-Polym. Phys.* **48**, 2148-2153 (2010).
7) Ion beam irradiation effects on resist materials, T. Gowa, T. Takahashi, T. Oka, T. Murakami, A. Oshima, S. Tagawa, and M. Washio, *J. Photopolym Sci. Technol.* **23**, 399-404 (2010).
8) OH radical in water studied by quantum beats on positron annihilation, J. J. Lee, T. Oka, and T. Hirade, *J. Phys.Conf. Ser.* **225**, 012030-1-012030-5 (2010).
9) Protective effects of silybin and analogues against X-ray radiation-induced damage, H. Fu, M. Lin, Y. Katsumura, A. Yokoya, K. Hata, Y. Muroya, K. Fujii, and N. Shikazono, *Acta Biochim. Biophys. Sin.* **42**, 489-495 (2010).
10) X-ray absorption spectra for nucleotides (AMP, GMP, and CMP) in liquid water solutions near the nitrogen K-edge, M. Ukai, A. Yokoya, K. Fujii, and Y. Saitoh, *Chem. Phys. Let.* **495**, 90-95 (2010).
11) Radiation chemical reactions in water radiolysis with therapeutic heavy ion beams, S. Yamashita, *Rad. Chem.* **90**, 11-16 (2010) (*in Japanese*).
12) Selective damage induction of DNA induced by monochromatic soft X-rays, K. Fujii, *Rad. Chem.* **90**, 17-22 (2010) (*in Japanese*).
13) Electron paramagnetic resonance study of unpaired electron species in thin films of pyrimidine bases by nitrogen and oxygen K-shell photoabsorption, T. Oka, A. Yokoya, and K. Fujii, *Appl. Phys. Lett.* **98**, 103701-1- 103701 -3 (2011).
14) Changes to the chemical structure of isotactic-polypropylene induced by ion-beam irradiation, T. Oka, A. Oshima, R. Motohashi, N. Seto, Y. Watanabe, R. Kobayashi, K. Saito, T. Murakami, M. Washio, and Y. Hama, *Radiat. Phys. Chem.* **80**, 278-280 (2011).
15) Study on depth profile of heavy ion irradiation effects in poly(tetrafluoroethylene-co-ethylene), T. Gowa, T. Shiotsu, T. Urakawa, T. Oka, T. Murakami, A. Oshima, Y. Hama, and M. Washio, *Radiat. Phys. Chem.* **80**, 264-267 (2011).
16) Ortho-positronium reactions in water studied by positron annihilation age-momentum correlation, T. Hirade, T. Oka, and J. J. Lee, *Materials Sci. Forum* **666**, 103-108 (2011).

Books & Reviews
1) Prologue: Untapped capability of radiation chemistry in radiation biology, S. Yamashita, *Rad. Chem.* **89**, 2 (2010) (*in Japanese*).
2) Epilogue: Pivotal issues of chemistry and biology in radiation sciences, A. Yokoya, *Rad. Chem.* **89**, 36-37 (2010) (*in Japanese*).
3) Chap. 20: Spectroscopic study of radiation-induced DNA lesions and their susceptibility to enzymatic repair, A. Yokoya, K. Fujii, N. Shikazono, and M. Ukai, *In* Charged Particle and Photon Interactions with Matter - Recent Advances, Applications, and Interfaces -, ed. by Y. Hatano, Y. Katsumura, and A. Mozumder, CRC Press, 543-574, (2011).
4) Chap. 13: Radiation chemistry of liquid water with heavy ions: steady-state and pulse radiolysis studies, S. Yamashita, M. Taguchi, G., and Y. Katsumura, Baldacchino, *In* Charged Particle and Photon Interactions with Matter - Recent Advances, Applications, and Interfaces -, ed. by Y. Hatano, Y. Katsumura, and A. Mozumder, CRC Press, 325-354, (2011).

Invited Talks
1) Improvement of radiation resistance of polymers by inorganic coating, Y. Kobayashi, T. Oka and Y. Hama, *International Workshop on Radiation Effects in Nuclear Technology*, Tokyo, Japan (2011).
2) Fabrication of functionally gradient PEM using heavy ion beams grafting, M. Washio, F. Shiraki, Y. Oshima, Y. Takasawa, H. Fujita, T. Gowa, H. Kudo, T. Oka, Y. Hama, T. Murakami, and A. Oshima, *The 2010 International Chemical Congress of Pacific Basin Societies (Pacifichem 2010)*, Hawaii, USA (2010).
3) A. Yokoya. Various modes of DNA damage formation by the direct effect of radiation. *The 56th Annual Meeting of Radiation Research Society*, Hawaii, USA (2010).
4) Water radiolysis with high-energy heavy ions: conversion of transient water radicals into stable product inside heavy-ion tracks. Symposium on bridging the gap between track structure and stable end products, S. Yamashita, Y. Katsumura, J. Meesungnoen, J.-P. Jay-Gerin, M. Lin, Y. Muroya and T. Murakami, *The 56th Annual Meeting of Radiation Research Society*, Hawaii, USA (2010).

Research Group for Spin-Polarized Positron Beam

Papers
1) Spin-polarized positron annihilation measurements on polycrystalline Fe, Co, Ni and Gd based on Doppler broadening of annihilation radiation, A. Kawasuso, M. Maekawa, Y. Fukaya. A. Yabuuchi, and I. Mochizuki, *Phys. Rev.* B **83**, 100406(R)-1-100406(R)-4 (2011).
2) Defect Structure of MBE-grown GaCrN Diluted Magnetic Semiconductor Film, A. Yabuuchi, M. Maekawa, A. Kawasuso, S. Hasegawa,, Yi-Kai Zhou, and H. Asahi, *J. Phys. Conf. Ser.* **262**, 012066-1-012066-4 (2011).
3) Positron Microbeam Study on Vacancy Generation Caused by Stress Corrosion Crack Propagation in Austenitic Stainless Steels, A. Yabuuchi, M. Maekwa, and A. Kawasuso, *J. Phys. Conf. Ser.* **262**, 012067-1-012067-4 (2011).
4) Development of spinpolarized positron beam using high energy proton beam, M. Maekawa, A. Kawasuso, Y. Fukaya, and A. Yabuuchi, *J. Phys. Conf. Ser.* **262**, 012035-1-012035-4 (2011).
5) A study of defects in electron- and ion-irradiated ZrCuAl bulk glassy alloy using positron annihilation techniques, F. Hori, N. Onodera, Y. Fukumoto, A. Ishii, A. Iwase, A. Kawasuso, A. Yabuuchi, M. Maekawa, and Y. Yokoyama, *J. Phys. Conf. Ser.* **262**, 012025-1-012025-4 (2011).
6) Electron compound nature in a surface atomic layer of a two-dimensional hexagonal lattice, I. Matsuda, F. Nakamura, K.Kubo, T. Hirahara, S. Yamazaki, W. H. Choi, H. W. Yeom, H. Narita, Y. Fukaya, M. Hashimoto, A. Kawasuso, M. Ono, Y. Hasegawa, S. Hasegawa, and K. Kobayashi, *Phys. Rev.* B **82**,165330-1-165330-6 (2010).
7) Spin conversion of positronium in NiO/Al_2O_3 catalysts observed by coincidence Doppler broadening technique, H.J. Zhang, Z. Q. Chen, S. J. Wang, A. Kawasuso, and N. Morishita, *Phys. Rev.* B **82**, 035439-1-035439-10 (2010).
8) Free volume in Zr-based bulk glassy alloys studied by positron annihilation techniques, A Ishii, A. Iwase Y. Yokoyama, T. J. Konno, A. Kawasuso, A Yabuuchi, M. Maekawa, and F. Hori, *J. Phys. Conf. Ser.* **225**, 012020-1-012020-4 (2010).
9) Surface plasmon excitation at metal surface studied by reflection high-energy positron diffraction, Y. Fukaya, A. Kawasuso and A. Ichimiya, *J. Phys. Conf. Ser.* **225**, 012009-1-012009-4 (2010).
10) Structure and phse transition of low-dimensional metals on crystal surface studied by reflection high-energy positron diffraction, Y. Fukaya, M. Hashimoto, A. Kawasuso, and A. Ichimiya, *J. Phys. Conf. Ser.* **225**, 012008-1-012008-4 (2010).
11) Free-volume structure of fluoropolymer-based radiationgrafted electrolyte membranes investigated by positron annihilation lifetime spectroscopy, S. Sawada, A. Kawasuso, M. Maekawa, A. Yabuuchi, and Y. Maekawa, *J. Phys. Conf. Ser.* **225**, 012048-1-012048-4 (2010).
12) Development of Spin-Polarized Positron Beam, A. Kawasuso, Y. Fukaya, M. Maekawa and A. Yabu-uchi, *J. Phys. Conf. Ser.* **225**, 012028-1-012028-4 (2010).
13) Coincidence Doppler broadening spectra of some single-element materials from the second to the sixth periods, A. Kawasuso, M. Maekawa, and K. Betsuyaku, *J. Phys. Conf. Ser.* **225**, 012027-1-012027-4 (2010).
14) Characterization of the Helium Bubbles in Si Probed by a Slow Positron Beam, M. Maekawa, A. Kawasuso, *J. Phys. Conf. Ser.* **225**, 012032-1-012032-4 (2010).
Application of positron microbeam for the meterials under the extreme condition, M. Maekawa, A. Yabuuchi, and A. Kawasuso, *J. Phys. Conf. Ser.* **225**, 012033-1-012033-4 (2010).
15) Surface plasmon excitation at topmost surface in reflection high-energy positron diffraction, Y. Fukaya, A. Kawasuso, and A. Ichimiya, *e-J. Surf. Sci. Nanotech.* **8**, 190-1-190-4 (2010).

Invited Talks
1) New Positron Beam Studies of Surface Low-Dimensional Systems and Magnetic Substances, A. Kawasuso, *12th International Workshop on Slow Positron Beam Techniques*, North Queensland, Australia (2010).

Researches conducted under collaborations between ASRC groups appear in each group's publication list. Excluding the overlap, the total number of Papers is 190.

Appendix

◆Pre-Review meeting : The Evaluation Committee of Research Activities for Advanced Science Research

Date: April 22-23, 2010
Committee

Chairperson	Takeshi Egami	UT-ORNL Distinguished Scientist/Professor, Department of Materials Science and Engineering, the University of Tennessee, USA
Committee members	Yasuhiro Ie	Director, the Institute for Solid State Physics, The University of Tokyo
	Sukekatsu Ushioda	President, National Institute for Materials Science
	Shigeo Koyasu	Professor, School of Medicin, Keio University
	Tatsuo Shikama	Head, International Research Center for Nuclear Materials Science, Institute for Materials Research, Tohoku University
	Kohei Tamao	Director, Advanced Science Institute, RIKEN
	Hiroshi Toki	Professor Emeritus, Osaka University
	Hidetoshi Fukuyama	Vice President, Tokyo University of Science
	Albert Fert	Scientific Director, the CNRS/ Thales Joint Physics Unit, Professor of Physics, University of Paris-Sud, Orsay, France Nobel Prize Winner in Physics 2007
	Peter Fulde	Director and Scientific Member, Max Planck Institute for the Physics of Complex Systems, Germany Director, Asia-Pacific Center for Theoretical Physics
	Norbert Trautmann	Honorary Professor, the Johannes Gutenberg University of Mainz, German

Pre Review Report : http://jolissrch-inter.tokai-sc.jaea.go.jp/pdfdata/JAEA-Evaluation-2010-006.pdf (PDF:2MB)

◆International Workshop

The 1st International ASRC Workshop on "New approach to the exotic phases of actinides compounds under unconventional experimental conditions"
Date : February 16-18, 2011
Venue : Advanced Science Research Center, Tokai, Japan
Organizers : G. H. Lander (ILL, France) and S. Kambe (JAEA)
URL : http://asrc.jaea.go.jp/soshiki/gr/kambe-gr/Workshop2011/Main.html

◆ASRC Seminar

No	Title	Speaker	Affiliation
386	Microbes and microbial products for nuclear waste remediation	Lynne Macaskie	University of Birmingham
	Bacterial transformations of radionuclides and metals	Joanna Renshaw	
387	Spintronics	Samuel D. Bader	Argonne National Laboratory (Advisor of ASRC)
388	Quantum criticality, and the physics and chemistry of superconductivity	Zachary Fisk	University of California, Irvine Invited Researcher for ASRC (Group Leader)
390	Quantum criticality in Yb-based compounds: thermal transport and Seebeck properties	Koichi Izawa	Tokyo Institute of Technology
391	Spin and charge dynamics in anti-ferromagnetic phase of iron-based superconductors	Takami Tohyama	Yukawa Institute for Theoretical Physics, Kyoto University
392	6th workshop of JAEA actinide network: Actinide solution chemistry and actinide nuclei NMR	Yasuhisa Ikeda	Tokyo Institute of Technology
		Toshiyuki Fujii	Kyoto University
		Akira Kirishima	Tohoku University
		Yoshihiro Kitatsuji	JAEA
		Hironori Sakai	JAEA
393	A prototype of kaonic nuclei K-pp	Akinobu Dote	High Energy Accelerator Research Orgnization (KEK)
394	Multi-nucleon transfer reactions in low-energy collisions of heavy ions	Valery Zagrebaev	Flerov Laboratory of Nuclear Reactions
395	Solid state theory for actinide compounds	Takashi Hotta	Tokyo Metropolitan University
396	K and Φ mesons in nuclear matter	Hiroaki Ohnishi	RIKEN
397	Variational cluster approximation for transition metal oxides	Robert Eder	Chiba University Karlsruhe Institute of Technology
398	Anomalous magnetic properties of transition metal chains from first-principles calculations	Guang-Yu Guo	Department of Physics, National Taiwan University
	Majorana fermion in topological superconductors	Naoto Nagaosa	The University of Tokyo
399	Analysis of Fe-based superconductors using 5-orbital model toward microscopic understanding of heavy fermion state	Hiroaki Ikeda	Kyoto University
	Parity-mixed superconductivity in non-centrosymmetric superconductors and non-Fermi liquid behaviors in electron scattering.	Tetsuya Takimoto	Asia Pacific Center for Theoretical Physics
400	Experimental study of Quark Gluon Plasma at RHIC	Yasuyuki Akiba	RIKEN
401	Unusual elecronic phases of Mott insulators with strong spin-orbit coupling	Giniyatulla Khaliullin	Max-Planck-Institute
402	Electromotive force induced by zinc-blende MnAs nanomagnets	Pham Nam Hai	The University of Tokyo

403	Issues in correlated electron actinide materials	Zachary Fisk	University of California,Irvine Invited Researcher for ASRC (Group Leader)
404	MuSR studies of doped magnetic semiconductor (Ga,Mn) As and development of a next generation system Li (Zn,Mn) As	Yasutomo J.Uemura	Columbia University
405	The start of superheavy element research at TASCA	Matthias Schädel	GSI Invited Researcher for ASRC (Group Leader)
406	Spin current induced phenomena in nano-structures	Yoshichika Otani Yasuhiro Niimi Dahai Wei	The University of Tokyo
407	New approach of magnetic resonance toward nano-meter resolution	Yosuke Yoshinari	JEOL Ltd.
408	Gain of the kinetic energy of bipolarons in the t-J-Holstein model based on electron-phonon coupling	Janez Bonca	Jozef Stefan Institute
409	Recent and future research on superheavy elements at Mainz/GSI	Jens V. Kratz	The Johannes Gutenberg University of Mainz
411	A study of Ξ production in (K-, K+) reactions by semi-classical distorted wave approximation and Ξ-nucleus potential	Shintaro Hashimoto	Post-Doctoral Fellow, JAEA
412	Electromotive force in magnetic tunnel junctions	Hyun-Woo Lee	Pohang University of Science and Technology
413	Multifunctional properties in heusler compounds:from topological insulators to spintronics	Claudia Felser	The Johannes Gutenberg University of Mainz
414	Selected topics in spin caloritronics	Gerrit E. W. Baure	Delft University of Technology
415	The transport coefficients for the large scale nuclear collective motion	Fedir A. Ivanyuk	Kiev Institute for Nuclear Reseach
416	NMR imaging -technology and its development in Japan	Hiroshi Yasuoka	JAEA
417	Hypernuclear weak decay measurements with FINUDA experiment	Simonetta Marcello	University of Turin
418	Magnetic interactions and excitations in multiferroic $MnWO_4$	Timothy Ziman	Institute Laue-Langevin
419	Spin spirals in underdoped cuprates:theory and experiment	Oleg P. Sushkov	University of New South Wales
420	Numerical study of interacting systems driven by a constant electric field	Janez Bonca	Jozef Stefan Institute
421	Spin current and spintronics	Koki Takanashi	Institute for Materials Research, Tohoku University
422	Development of the quantum-mechanical method suitable for systems with 20000 atoms	Dmitri Fedorov	Advanced Industrial Science and Technology
423	A Tale of two oxygens: Two types of oxygens in high-Tc cuprates observed by STM	Shin-ichi Uchida	Graduate School of Science, The University of Tokyo
424	Exotic charmed hadrons and charmed nuclei	Shigehiro Yasui	High Energy Accelerator Research Organization (KEK)
425	Radiation and pgoto-induced oxidative DNA damage	Kiyohiko Kawai	The institute of Scientific and Industrial Research, Osaka University
426	Matrix product state in discretized and continuous space -Density renormalization group, Bethe ansatz, Z2 topological invariant-	Isao Maruyama	Graduate School of Engineering Science, Osaka University
427	Exotic atom and molecule including supersymmetric tau particles and catalyzed nuclear fusion	Yasushi Kino	Faculty of Science, Tohoku University
428	Sp scattering experiment project at J-PARC	Kouji Miwa	Graduate School of Science, Tohoku Univeristy
430	The transport coefficients for the large scale nuclear collective motion	Fedir A. Ivanyuk	Institute for Nuclear Research
434	Molecular spintronics: Spin polarized transport through quantum dots and molecules	Jan Martinek	Polish Academy of Sciences
435	Nonequilibrium quantum dynamics of a charge carrier doped into Mott insulator	Lev Vidmar	Jozef Stefan Institute

◆Research theme accepted for Reimei Research Program

Research Theme	Project Director (Applicant)	Organization
New approach to the exotic phases of actinides compounds under unconventional experimental conditions	Gerry H. Lander	Institut Laue-Langevin
Biological assessment of radaiation damage of ATP by Soft X-rays	Nobuyoshi Akimitsu	Radioisotope Center,The University of Tokyo
Theory of Materials for Spin Electronics and Dynamics of Magnetic Nanostructures	Timothy Ziman	Institut Laue-Langevin
Synthesis, MuSR and other studies of Li(Mn, Zn)As and I-II-V doped magnetic semiconductors	Yasutomo J. Uemura	Columbia University
Time-resolved neutron contrast method by pulse-magnetic-field nuclear polorization	Yasuo Narumi	Institute for Materials Research, Tohoku University

◆Research Collaborations and Cooperation

The number of Research collaborations	
Research collaborations	33
Research cooperations	3

The number of organizations based on joint research arrangement		
Domestic	Universities	19
	Public Institutions	6
	Others	7
Foreign Institutions		9

◆Visitors (the total number)

287